NASA Contractor Report 181659

ICASE REPORT NO. 88-27

ICASE

ON THE PREDICTION OF EQUILIBRIUM STATES IN HOMOGENEOUS TURBULENCE

Charles G. Speziale

Nessan Mac Giolla Mhuiris

Contract No. NAS1-18107
April 1988

INSTITUTE FOR COMPUTER APPLICATIONS IN SCIENCE AND ENGINEERING
NASA Langley Research Center, Hampton, Virginia 23665

Operated by the Universities Space Research Association

National Aeronautics and
Space Administration

Langley Research Center
Hampton, Virginia 23665

ON THE PREDICTION OF EQUILIBRIUM STATES IN HOMOGENEOUS TURBULENCE

Charles G. Speziale and Nessan Mac Giolla Mhuiris

Institute for Computer Applications in Science and Engineering
NASA Langley Research Center
Hampton, VA 23665

ABSTRACT

A comparison of several commonly used turbulence models (including the $K-\varepsilon$ model and two second-order closures) is made for the test problem of homogeneous turbulent shear flow in a rotating frame. The time evolution of the turbulent kinetic energy and dissipation rate is calculated for a variety of models and comparisons are made with previously published experiments and numerical simulations. Particular emphasis is placed on examining the ability of each model to accurately predict equilibrium states for a range of the parameter Ω/S (the ratio of the rotation rate to the shear rate). It is found that none of the commonly used second-order closure models yield substantially improved predictions for the time evolution of the turbulent kinetic energy and dissipation rate over the somewhat defective results obtained from the simpler K$-\varepsilon$ model for the turbulent flow regime. There is also a problem with the equilibrium states predicted by the various models. For example, the K$-\varepsilon$ model erroneously yields equilibrium states that are independent of Ω/S while the Launder, Reece, and Rodi model predicts a flow relaminarization when $\Omega/S > 0.39$ – a result which is contrary to numerical simulations and linear spectral analyses which indicate flow instability for at least the range $0 \leq \Omega/S \leq 0.5$. The physical implications of the results obtained from the various turbulence models considered herein are discussed in detail along with proposals to remedy the deficiencies based on a dynamical systems approach.

This research was supported by the National Aeronautics and Space Administration under NASA Contract No. NAS1-18107 while the authors were in residence at ICASE, NASA Langley Research Center, Hampton, VA 23665.

1. INTRODUCTION

Homogeneous turbulent flows have played a central role in the calibration and testing of a variety of turbulence models. The reason for this prominence is twofold: (a) homogeneous turbulence contains many of the important flow effects of scientific and engineering interest in a simplified setting which quite often gives rise to closed form solutions in the commonly used turbulence models, and (b) there is an abundance of reliable data from physical and numerical experiments with which to compare the predictions of turbulence models. In particular, the physical and numerical experiments on homogeneous plane shear and plane strain (see Tucker and Reynolds 1968, Champagne, Harris, and Corrsin 1970, Tavoularis and Corrsin 1981, and Rogallo 1981) have been used extensively in the calibration of second-order closure models and the most recent two-equation models of the K$-\varepsilon$ type. When a two-equation turbulence model or a second-order closure model is applied to homogeneous turbulence, it gives rise to an initial value problem for a set of coupled nonlinear ordinary differential equations – a dynamical systems problem. However, there appear to have been no previously published studies of homogeneous turbulence modeling from this nonlinear dynamics standpoint. This forms the motivation for the present study.

In this paper the performance of four commonly used turbulence models (the standard K$-\varepsilon$ model, a nonlinear $K-\varepsilon$ model, the Launder, Reece, and Rodi second-order closure model, and the Rotta-Kolmogorov second-order closure model) are examined for the test problem of homogeneous turbulent shear flow in a rotating frame – a problem which encompasses arbitrary combinations of plain strain and plane rotation. The time evolution of the turbulent kinetic energy and dissipation rate will be computed along with equilibrium states which, mathematically, are the fixed points of the resulting system of nonlinear ordinary differential equations. Extensive comparisons with physical and numerical experiments will be made. The results obtained are somewhat disappointing at least in a quantitative sense. For example, it will be shown that the commonly used two-equation models of the K$-\varepsilon$ type yield predictions for the turbulent kinetic energy and dissipation

rate that are independent of the state of rotation of the fluid – a result which is in substantial contradiction to numerical simulations of the Navier-Stokes equations. While the second-order closure models do yield rotationally dependent solutions, it will be shown that their predictions of the time evolution of the turbulent kinetic energy and dissipation rate are not (for the turbulent flow regime) substantially better than the significantly simpler K$-\varepsilon$ model. Considerable attention will be paid to the ability of each model to predict equilibrium states. In this regard, it will be shown that there are deficiencies in the commonly used second-order closures. For example, the Launder, Reece, and Rodi model will be shown to predict a flow relaminarization when $\Omega/S > 0.39$ whereas large-eddy simulations and linear spectral analyses indicate that there is an exponential growth in the turbulent kinetic energy and dissipation rate for $0 \leq \Omega/S \leq 0.5$ (it is only their ratio, the turbulent time scale, that approaches a structural equilibrium). On the other hand, the K$-\varepsilon$ model erroneously predicts unstable flow for all values of Ω/S with exactly the same turbulence structure. The results predicted by these four turbulence models will be documented in detail and specific proposals will be made for the development of improved models.

2. TURBULENT SHEAR FLOW IN A ROTATING FRAME

We will consider the problem of homogeneous turbulent shear flow in a steadily rotating frame for an incompressible viscous fluid (see Figure 1). This problem is chosen because it incorporates arbitrary combinations of plane rotations and strains and, hence, represents a rather general class of homogeneous turbulent flows in a simplified setting. Since the homogeneous turbulence problem being considered is planar, the Reynolds equation is satisfied identically for all values of the rotation rate Ω and shear rate S (c.f., Reynolds 1987). Consequently, no consistency problems can arise since the mean momentum and continuity equations are satisfied identically for the entire range of parameter space. For the problem at hand, the mean velocity gradient tensor is given by

$$\frac{\partial \overline{v}_i}{\partial x_j} = \begin{pmatrix} 0 & S & 0 \\ 0 & 0 & 0 \\ 0 & 0 & 0 \end{pmatrix} \tag{1}$$

and $\Omega_i = (0, 0, \Omega)$ is the rotation rate of the framing relative to an inertial frame of reference. We will restrict our attention to incompressible fluids with constant properties.

First, we will consider the traditional K$-\varepsilon$ model for which the turbulent kinetic energy K and dissipation rate ε are solutions of the nonlinear ordinary differential equations (see Hanjalic and Launder 1972)

$$\dot{K} = \tau_{ij} \frac{\partial \overline{v}_i}{\partial x_j} - \varepsilon \tag{2}$$

$$\dot{\varepsilon} = C_{\varepsilon 1} \frac{\varepsilon}{K} \tau_{ij} \frac{\partial \overline{v}_i}{\partial x_j} - C_{\varepsilon 2} \frac{\varepsilon^2}{K} \tag{3}$$

for any homogeneous turbulent flow. Here, τ_{ij} is the Reynolds stress tensor (such that $K = -\frac{1}{2}\tau_{ii}$) which is represented by the eddy viscosity model

$$\tau_{ij} = -\frac{2}{3} K \delta_{ij} + C_\mu \frac{K^2}{\varepsilon} \left(\frac{\partial \overline{v}_i}{\partial x_j} + \frac{\partial \overline{v}_j}{\partial x_i} \right) \tag{4}$$

where C_μ, $C_{\varepsilon 1}$, and $C_{\varepsilon 2}$ are constants which are usually taken to assume the values of 0.09, 1.45, and 1.90, respectively. For turbulent shear flow in a rotating frame, equations (2) - (3) simplify to

$$\dot{K} = C_\mu \frac{K^2}{\varepsilon} S^2 - \varepsilon \tag{5}$$

$$\dot{\varepsilon} = C_{\varepsilon 1} C_\mu K S^2 - C_{\varepsilon 2} \frac{\varepsilon^2}{K} \tag{6}$$

and the components of the anisotropy tensor $b_{ij} \equiv -(\tau_{ij} + \frac{2}{3} K \delta_{ij})/K$ are as follows

$$b_{11} = 0, \quad b_{12} = -C_\mu S K/\varepsilon, \quad b_{13} = 0 \tag{7}$$

$$b_{22} = 0, \quad b_{23} = 0, \quad b_{33} = 0. \tag{8}$$

Equations (5) - (6) can be combined to yield a nonlinear differential equation for ε/SK of the form

$$\frac{d}{d\tau}\left(\frac{\varepsilon}{SK}\right) = C_\mu(C_{\varepsilon 1} - 1) - (C_{\varepsilon 2} - 1)\left(\frac{\varepsilon}{SK}\right)^2 \tag{9}$$

where $\tau = St$ is the dimensionless time. The time evolution of the anisotropy tensor can be obtained from (7) - (9) which are solved subject to the initial condition

$$\frac{\varepsilon}{SK} = \frac{\varepsilon_0}{SK_0} \tag{10}$$

at time $\tau = 0$. Then, the turbulent kinetic energy can be obtained from Eq. (5) integrated in the form

$$\frac{d}{d\tau}\left(\frac{K}{K_0}\right) = \left(C_\mu \frac{SK}{\varepsilon} - \frac{\varepsilon}{SK}\right)\left(\frac{K}{K_0}\right) \tag{11}$$

which constitutes a linear differential equation for K/K_0 once ε/SK is determined from (9). Here, $\varepsilon/\varepsilon_0$ can be easily obtained once K/K_0 and ε/SK are known since

$$\frac{\varepsilon}{\varepsilon_0} = \frac{SK_0}{\varepsilon_0}\left(\frac{K}{K_0}\right)\left(\frac{\varepsilon}{SK}\right). \tag{12}$$

It therefore follows that the evolution of K/K_0, $\varepsilon/\varepsilon_0$, and SK/ε in time τ only depends on the shear rate and initial conditions through the dimensionless parameter SK_0/ε_0. Consequently, the K$-\varepsilon$ model predicts that two homogeneous turbulent shear flows are dynamically similar provided that SK_0/ε_0 are the same for both flows. This is only partially consistent with the Navier-Stokes equations which at least require that both SK_0/ε_0 and the shape of the initial energy spectrum be the same for two flows to be dynamically similar. The equations of motion for the K$-\varepsilon$ model in homogeneous turbulent

shear flow are the same in *all* frames of reference independent of whether or not they are inertial and, therefore, the time evolution of K/K_0, $\varepsilon/\varepsilon_0$, and SK/ε are independent of the rotation rate Ω of the reference frame. This result will be shown later to be in serious disagreement with numerical simulations of the Navier-Stokes equations.

Equation (9) has an equilibrium solution (in the limit as $\tau \to \infty$) which is of the form

$$\left(\frac{SK}{\varepsilon}\right)_\infty = \left(\frac{\alpha}{C_\mu}\right)^{\frac{1}{2}} \tag{13}$$

where $\alpha \equiv (C_{\varepsilon 2} - 1)/(C_{\varepsilon 1} - 1)$. Hence, the long time solutions (i.e., when $\tau \gg 1$) for K/K_0 and $\varepsilon/\varepsilon_0$ behave as

$$K \sim \exp\left[\sqrt{\frac{C_\mu}{\alpha}}\left(\sqrt{\alpha} - 1\right)\tau\right] \tag{14}$$

$$\varepsilon \sim \exp\left[\sqrt{\frac{C_\mu}{\alpha}}\left(\sqrt{\alpha} - 1\right)\tau\right] \tag{15}$$

which are obtained by substituting (13) into (11) and (12). It is thus clear that the K$-\varepsilon$ model predicts that there is an exponential growth of K and ε in time for homogeneous turbulent shear flow; a structural equilibrium is reached in their dimensionless ratio SK/ε which is completely independent of initial conditions. It is encouraging to note that this physical picture is consistent with direct numerical simulations of the Navier-Stokes equations (see Rogallo 1981) and physical experiments (see Tavoularis and Corrsin 1981) for turbulent shear flow in an inertial framing.

Speziale (1987) recently proposed a nonlinear $K-\varepsilon$ model which, for turbulent channel and duct flows, was shown to yield dramatically improved predictions for the normal Reynolds stress anisotropies. The Reynolds stress tensor for this nonlinear $K-\varepsilon$ model generalized for rotating flows is as follows (see Speziale 1988)

$$\tau_{ij} = -\frac{2}{3}K\delta_{ij} + 2C_\mu\frac{K^2}{\varepsilon}\overline{S}_{ij} - 4C_\mu^2 C_D\frac{K^3}{\varepsilon^2}\left(\overset{\circ}{\overline{S}}_{ij} + \overline{S}_{ik}\overline{S}_{kj} - \frac{1}{3}\overline{S}_{mn}\overline{S}_{mn}\delta_{ij} + 2\overline{W}_{ik}\overline{S}_{kj} + 2\overline{W}_{jk}\overline{S}_{ki}\right) \tag{16}$$

where

$$\overset{\circ}{\overline{S}}_{ij} \equiv \frac{\partial \overline{S}_{ij}}{\partial t} + \overline{\boldsymbol{v}} \cdot \nabla \overline{S}_{ij} - \overline{\omega}_{ik}\overline{S}_{kj} - \overline{\omega}_{jk}\overline{S}_{ki} \tag{17}$$

$$\overline{\omega}_{ij} \equiv \frac{1}{2}\left(\frac{\partial \overline{v}_i}{\partial x_j} - \frac{\partial \overline{v}_j}{\partial x_i}\right) \tag{18}$$

$$\overline{W}_{ij} \equiv \overline{\omega}_{ij} + \varepsilon_{mji}\Omega_m \tag{19}$$

are, respectively, the frame-indifferent Jaumann derivative of $\overline{\mathbf{S}}$, the mean vorticity tensor, and the intrinsic mean vorticity tensor (i.e., the mean vorticity tensor relative to an inertial framing). It is clear that the traditional $K-\varepsilon$ model is extracted in the limit as $C_D \to 0$ (C_D was evaluated to be 1.68 by correlating with experimental data for turbulent channel flow; see Speziale 1987). Equation (16) must be solved in conjunction with modeled transport equations for the turbulent kinetic energy and dissipation rate. The same transport equations for K and ε as developed for the traditional $K-\varepsilon$ model (see equations (2) - (3)) have been used for simplicity. Consequently, for homogeneous turbulent shear flow in a rotating frame, it can be shown that

$$b_{11} = C_D C_\mu^2 \left(\frac{SK}{\varepsilon}\right)^2 \left[\frac{7}{3} - 8\left(\frac{\Omega}{S}\right)\right], \quad b_{12} = -C_\mu \frac{SK}{\varepsilon} \tag{20}$$

$$b_{22} = C_D C_\mu^2 \left(\frac{SK}{\varepsilon}\right)^2 \left[-\frac{5}{3} + 8\left(\frac{\Omega}{S}\right)\right], \quad b_{33} = -\frac{2}{3} C_D C_\mu^2 \left(\frac{SK}{\varepsilon}\right)^2 \tag{21}$$

for the nonlinear $K-\varepsilon$ model. Since b_{12} is of the same form for both the nonlinear and linear $K-\varepsilon$ model, it follows that the transport equations for K and ε corresponding to (20) and (21) are the same as their linear counterparts. More specifically, equations (20) - (21) are solved along with the transport equations (5) - (6) which yield the *same* results for K and ε as obtained from the traditional $K-\varepsilon$ model (most notably, this means that the equilibrium value of $(SK/\varepsilon)_\infty = \sqrt{\alpha/C_\mu}$ is the same as given in equation (13) for the traditional K$-\varepsilon$ model). Hence, the nonlinear K$-\varepsilon$ model of Speziale (1987, 1988) only gives rise to differences in the normal components of the anisotropy tensor. Later, it will be shown how these differences constitute a substantial improvement over the traditional K$-\varepsilon$ model.

The most popular second-order closure model currently used is that of Launder, Reece, and Rodi (1975). In the most commonly used form of this model, the Reynolds stress

tensor is a solution of the transport equation

$$\begin{aligned}\dot{\tau}_{ij} &= (C_2-1)\left(\tau_{ik}\frac{\partial \overline{v}_j}{\partial x_k}+\tau_{jk}\frac{\partial \overline{v}_i}{\partial x_k}\right)+(C_2-2)(\tau_{ik}\epsilon_{mkj}\Omega_m \\ &+\tau_{jk}\epsilon_{mki}\Omega_m)-C_1\frac{\varepsilon}{K}(\tau_{ij}+\frac{2}{3}K\delta_{ij}) \\ &-\frac{2}{3}C_2\tau_{k\ell}\frac{\partial \overline{v}_k}{\partial x_\ell}\delta_{ij}+\frac{2}{3}\varepsilon\delta_{ij}\end{aligned} \tag{22}$$

which has been simplified for any rotating homogeneous turbulence. In equation (22), C_1 and C_2 are empirical constants which assume the values of 1.8 and 0.6, respectively. This Reynolds stress transport model is solved in conjunction with the modeled dissipation rate equation given by (3) where $C_{\varepsilon 1}=1.45$ and $C_{\varepsilon 2}=1.90$. For the problem of homogeneous turbulent shear flow in a rotating frame, the Launder, Reece, and Rodi model yields the following system of coupled nonlinear ordinary differential equations:

$$\dot{K}=\tau_{12}S-\varepsilon \tag{23}$$

$$\dot{\varepsilon}=C_{\varepsilon 1}\frac{\varepsilon}{K}\tau_{12}S-C_{\varepsilon 2}\frac{\varepsilon^2}{K} \tag{24}$$

$$\dot{\tau}_{12}=\tau_{22}S+(C_2-2)[\Omega\tau_{11}+\tau_{22}(S-\Omega)]-C_1\frac{\varepsilon}{K}\tau_{12} \tag{25}$$

$$\dot{\tau}_{11}=2\tau_{12}S+2(C_2-2)(S-\Omega)\tau_{12}-C_1\frac{\varepsilon}{K}(\tau_{11}+\frac{2}{3}K)-\frac{2}{3}C_2\tau_{12}S+\frac{2}{3}\varepsilon \tag{26}$$

$$\dot{\tau}_{22}=2\Omega(C_2-2)\tau_{12}-C_1\frac{\varepsilon}{K}(\tau_{22}+\frac{2}{3}K)-\frac{2}{3}C_2\tau_{12}S+\frac{2}{3}\varepsilon \tag{27}$$

Since

$$\tau_{33}=-(\tau_{11}+\tau_{22}+2K) \tag{28}$$

it is not necessary to solve the transport equation for τ_{33}. The system of equations (23) - (27) can be non-dimensionalized and recast into an alternative system of equations for ε/SK, b_{11}, b_{12}, b_{22}, and K/K_0 which are as follows:

$$\frac{d}{d\tau}\left(\frac{\varepsilon}{SK}\right)=(1-C_{\varepsilon 1})(\frac{\varepsilon}{SK})b_{12}+(1-C_{\varepsilon 2})\left(\frac{\varepsilon}{SK}\right)^2 \tag{29}$$

$$\frac{d}{d\tau}\left(\frac{K}{K_0}\right)=-\left(b_{12}+\frac{\varepsilon}{SK}\right)\left(\frac{K}{K_0}\right) \tag{30}$$

$$\frac{db_{12}}{d\tau} = (C_2 - 1)\left(b_{22} + \frac{2}{3}\right) + (C_2 - 2)\left[\frac{\Omega}{S}(b_{11} - b_{22})\right] - (C_1 - 1)\left(\frac{\varepsilon}{SK}\right) b_{12} + b_{12}^2 \qquad (31)$$

$$\frac{db_{11}}{d\tau} = 2\left[(2 - C_2)\frac{\Omega}{S} + \frac{2}{3}(C_2 - 1)\right] b_{12} + (1 - C_1)\left(\frac{\varepsilon}{SK}\right) b_{11} + b_{12}b_{11} \qquad (32)$$

$$\frac{db_{22}}{d\tau} = 2\left[(C_2 - 2)\frac{\Omega}{S} - \frac{1}{3}(C_2 - 1)\right] b_{12} + (1 - C_1)\left(\frac{\varepsilon}{SK}\right) b_{22} + b_{12}b_{22} \qquad (33)$$

where $\tau = St$ is the dimensionless time. These nonlinear ordinary differential equations are solved subject to the initial conditions

$$\frac{\varepsilon}{SK} = \frac{\varepsilon_0}{SK_0}, \quad b_{11} = 0, \quad b_{12} = 0, \quad b_{22} = 0 \qquad (34)$$

at time $\tau = 0$ which correspond to a state of isotropy (the same conditions that are usually taken in physical and numerical experiments). It should be noted that b_{33} and $\varepsilon/\varepsilon_0$ can be obtained from the computed variables as follows

$$\frac{\varepsilon}{\varepsilon_0} = \frac{\varepsilon}{SK}\left(\frac{SK_0}{\varepsilon_0}\right)\left(\frac{K}{K_0}\right) \qquad (35)$$

$$b_{33} = -(b_{11} + b_{22}). \qquad (36)$$

It is also interesting to note that the shear rate only enters into the solution of the problem through the initial condition SK_0/ε_0. Hence, there can be equilibrium solutions which only depend on a single parameter – the ratio of the rotation rate to the shear rate Ω/S. Such equilibrium states are of the form

$$\frac{\varepsilon}{SK} = \left(\frac{\varepsilon}{SK}\right)_\infty, \quad b_{11} = (b_{11})_\infty, \quad b_{12} = (b_{12})_\infty, \quad b_{22} = (b_{22})_\infty \qquad (37)$$

in the limit as $\tau \to \infty$. In dynamical systems terms, (37) constitute the fixed points in the four dimensional phase space (ε/SK, b_{11}, b_{12}, b_{22}) of equations (29), (31), (32) and (33). Mathematically, these fixed points are determined by setting the time derivatives of ε/SK, b_{11}, b_{12}, and b_{22} to zero. This yields the nonlinear system of algebraic equations

$$\frac{\varepsilon}{SK}\left[(1 - C_{\varepsilon 1})b_{12} + (1 - C_{\varepsilon 2})\left(\frac{\varepsilon}{SK}\right)\right] = 0 \qquad (38)$$

$$(C_2-1)\left(b_{22}+\frac{2}{3}\right)+(C_2-2)\left[\frac{\Omega}{S}(b_{11}-b_{22})\right]-(C_1-1)\frac{\varepsilon}{SK}b_{12}+b_{12}^2=0 \qquad (39)$$

$$2\left[(2-C_2)\frac{\Omega}{S}+\frac{2}{3}(C_2-1)\right]b_{12}+(1-C_1)\left(\frac{\varepsilon}{SK}\right)b_{11}+b_{12}b_{11}=0 \qquad (40)$$

$$2\left[(C_2-2)\frac{\Omega}{S}-\frac{1}{3}(C_2-1)\right]b_{12}+(1-C_1)\left(\frac{\varepsilon}{SK}\right)b_{22}+b_{12}b_{22}=0 \qquad (41)$$

whose solutions will be examined in the next section.

The Rotta-Kolmogorov model (c.f., Mellor and Herring 1973) will be the last model considered. Since this model has been applied to a variety of geophysical fluid dynamics problems involving system rotations (c.f., Mellor and Yamada 1974), its performance in predicting homogeneous turbulent shear flow in a rotating frame is of interest. For a general homogeneous turbulence in a rotating frame, the Rotta-Kolmogorov model takes the form

$$\begin{aligned}\dot{\tau}_{ij} &= -\tau_{im}\left(\frac{\partial\overline{v}_j}{\partial x_m}+2\varepsilon_{nmj}\Omega_n\right)-\tau_{jm}\left(\frac{\partial\overline{v}_i}{\partial x_m}+2\varepsilon_{nmi}\Omega_n\right)\\ &\quad -\frac{\sqrt{2}}{3A_1}\frac{K^{\frac{1}{2}}}{\ell}\left(\tau_{ij}+\frac{2}{3}K\delta_{ij}\right)-2C_1K\left(\frac{\partial\overline{v}_i}{\partial x_j}+\frac{\partial\overline{v}_j}{\partial x_i}\right)+\frac{4}{3}\frac{\sqrt{2}K^{\frac{3}{2}}}{B_1\ell}\delta_{ij} \qquad (42)\end{aligned}$$

$$\overline{K\ell}=\frac{E}{2}\ell\tau_{ij}\frac{\partial\overline{v}_i}{\partial x_j}-\frac{\sqrt{2}}{B_1}K^{\frac{3}{2}} \qquad (43)$$

where ℓ is the length scale of turbulence, and A_1, B_1, C_1, and E are empirical constants which assume the values of 0.78, 15.0, 0.056, and 1.4, respectively. For homogeneous turbulent shear flow in a rotating frame, (42) - (43) yield the following system of nonlinear ordinary differential equations:

$$\dot{K}=\tau_{12}S-\frac{2\sqrt{2}}{B_1}\frac{K^{\frac{3}{2}}}{\ell} \qquad (44)$$

$$\dot{\overline{K\ell}} = \frac{E}{2}\ell\tau_{12}S - \frac{\sqrt{2}}{B_1}K^{\frac{3}{2}} \tag{45}$$

$$\dot{\tau}_{12} = \frac{\sqrt{2}}{3A_1}\frac{K^{\frac{1}{2}}}{\ell}\tau_{12} - 2C_1KS - \tau_{22}S + 2\Omega(\tau_{22} - \tau_{11}) \tag{46}$$

$$\dot{\tau}_{11} = -\frac{\sqrt{2}}{3A_1}\frac{K^{\frac{1}{2}}}{\ell}(\tau_{11} + \frac{2}{3}K) - 2\tau_{12}(S - 2\Omega) + \frac{4\sqrt{2}}{3B_1}\frac{K^{\frac{3}{2}}}{\ell} \tag{47}$$

$$\dot{\tau}_{22} = -\frac{\sqrt{2}}{3A_1}\frac{K^{\frac{1}{2}}}{\ell}(\tau_{22} + \frac{2}{3}K) - 4\tau_{12}\Omega + \frac{4\sqrt{2}}{3B_1}\frac{K^{\frac{3}{2}}}{\ell}. \tag{48}$$

However, the decay of turbulent kinetic energy is governed by the equation

$$\dot{K} = \tau_{12}S - \varepsilon \tag{49}$$

which is a rigorous consequence of the Navier-Stokes equations for the homogeneous turbulent shear flow under consideration. A simple comparison of equations (44) and (49) yields

$$\ell = \frac{2\sqrt{2}}{B_1}\frac{K^{\frac{3}{2}}}{\varepsilon} \tag{50}$$

for the Rotta-Kolmogorov model. Hence, as with the Launder, Reece, and Rodi model, the system of equations (44) - (48) can be non-dimensionalized and recast into an equivalent set of equations for SK/ε, b_{11}, b_{12}, and b_{22} as follows:

$$\frac{d}{d\tau}\left(\frac{\varepsilon}{SK}\right) = \left(\frac{E}{2} - \frac{3}{2}\right)\frac{\varepsilon}{SK}b_{12} - \left(\frac{\varepsilon}{SK}\right)^2 \tag{51}$$

$$\frac{db_{12}}{d\tau} = 2(C_1 - \frac{1}{3}) - b_{22} + \left(1 - \frac{B_1}{6A_1}\right)\frac{\varepsilon}{SK}b_{12} - 2\frac{\Omega}{S}(b_{11} - b_{22}) + b_{12}^2 \tag{52}$$

$$\frac{db_{11}}{d\tau} = 4\left(\frac{\Omega}{S} - \frac{1}{3}\right)b_{12} + \left(1 - \frac{B_1}{6A_1}\right)\frac{\varepsilon}{SK}b_{11} + b_{12}b_{11} \tag{53}$$

$$\frac{db_{22}}{d\tau} = -2\left(2\frac{\Omega}{S} - \frac{1}{3}\right)b_{12} + \left(1 - \frac{B_1}{6A_1}\right)\frac{\varepsilon}{SK}b_{22} + b_{12}b_{22} \tag{54}$$

where $\tau \equiv St$ is the dimensionless time. This system of nonlinear ordinary differential equations is solved subject to the initial conditions (34) which correspond to an isotropic turbulence. As with the Launder, Reece, and Rodi model, K/K_0, $\varepsilon/\varepsilon_0$ and b_{33} are obtained from the computed variables using equations (30), (35), and (36) which are model independent. The equilibrium states corresponding to the Rotta-Kolmogorov model are obtained by setting the time derivatives to zero in (51) - (54) which yields the nonlinear algebraic equations

$$\left(\frac{E}{2} - \frac{3}{2}\right)\frac{\varepsilon}{SK}b_{12} - \left(\frac{\varepsilon}{SK}\right)^2 = 0 \tag{55}$$

$$2\left(C_1 - \frac{1}{3}\right) - b_{22} + \left(1 - \frac{B_1}{6A_1}\right)\frac{\varepsilon}{SK}b_{12} - 2\frac{\Omega}{S}(b_{11} - b_{22}) + b_{12}^2 = 0 \tag{56}$$

$$4\left(\frac{\Omega}{S} - \frac{1}{3}\right)b_{12} + \left(1 - \frac{B_1}{6A_1}\right)\frac{\varepsilon}{SK}b_{11} + b_{12}b_{11} = 0 \tag{57}$$

$$-2\left(2\frac{\Omega}{S} - \frac{1}{3}\right)b_{12} + \left(1 - \frac{B_1}{6A_1}\right)\frac{\varepsilon}{SK}b_{22} + b_{12}b_{22} = 0. \tag{58}$$

The equations of motion for the Rotta-Kolmogorov model are of the same general form as those for the Launder, Reece, and Rodi model (only the values of the coefficients are altered). Hence, both second-order closure models have the same topological properties. For example, both models have exponential long time growth behavior, i.e.,

$$K \sim \exp\left\{|(b_{12})_\infty + \left(\frac{\varepsilon}{SK}\right)_\infty| \, \tau\right\} \tag{59}$$

$$\varepsilon \sim \exp\left\{|(b_{12})_\infty + \left(\frac{\varepsilon}{SK}\right)_\infty| \, \tau\right\} \tag{60}$$

for $\tau \gg 1$ and $(\varepsilon/SK)_\infty > 0$[‡] (it should be noted that Tavoularis (1985) predicted such an exponential growth for the spatially evolving version of homogeneous turbulent shear flow obtained by a Galilean transformation). Furthermore, the bifurcation diagrams for the

[‡]For $(\varepsilon/SK)_\infty = 0$, it will be demonstrated later that K and ε can either grow or decay with time.

models are qualitatively similar. A comparison of the results predicted by each of these models with physical and numerical experiments will be made in the next section.

3. COMPARISON OF THE MODELS

First, we will present computed results for the time evolution of the turbulent kinetic energy and dissipation rate predicted by the various models. It should be noted that both the traditional and nonlinear K$-\varepsilon$ models yield the same results for the time evolution of K/K_0 and $\varepsilon/\varepsilon_0$ (the differences between the two models are in their predictions for the anisotropy tensor). Computations were conducted for a variety of values of Ω/S using a Runge-Kutta-Fehlburg numerical integration scheme. In Figure 2, the time evolution of the turbulent kinetic energy is shown for $\Omega/S = 0$ and an initial condition of $\varepsilon_0/SK_0 = 0.496$ (picked to agree with the large-eddy simulations of Bardina, Ferziger, and Reynolds 1983). From this figure it is clear that none of the turbulent closure models considered are in good agreement with the numerical simulations. All of the models badly underpredict the turbulent kinetic energy obtained from large-eddy simulations. Two observations are noteworthy: (a) there is no discernible difference between the predictions of the Launder, Reece, and Rodi model and the K$-\varepsilon$ model for $St \leq 8$, (b) the Rotta-Kolmogorov model appears to badly underpredict the turbulent kinetic energy after large elapsed times (at $St = 10$, it yields a value for the turbulent kinetic energy which is only approximately half of that predicted by the K$-\varepsilon$ and Launder, Reece, and Rodi models). Computed values of the turbulent dissipation rate are shown in Figure 3 for $\Omega/S = 0$ and an initial condition of $\varepsilon_0/SK_0 = 0.496$. All of the models yield results that are in a comparable range of one another but which dramatically underpredict the large-eddy simulations.

No direct comparisons with the experiments of Champagne, Harris, and Corrsin (1970) are made because of the uncertainty as to what the initial dissipation was in that study. Mild to moderate changes in the initial dissipation (reflected in the initial condition ε_0/SK_0) can yield dramatically different results for the time evolution of the turbulent kinetic energy and dissipation rate. In Figure 4, the time evolution of the turbulent kinetic energy is shown for the Launder, Reece, and Rodi model and the Rotta-Kolmogorov model (both computed with $\varepsilon_0/SK_0 = 0.28$) along with the K$-\varepsilon$ model (computed with

$\varepsilon_0/SK_0 = 0.35$). Each of these models yield results that are in good agreement with the large-eddy simulations conducted for $\varepsilon_0/SK_0 = 0.496$ originally shown in Figure 2. Thus, we have demonstrated that model predictions can be misleadingly forced into agreement with the results of physical or numerical experiments by an ad hoc adjustment of the initial conditions. It is, therefore, meaningless to make comparisons with such experiments unless the initial conditions are known with a strong degree of certainty. Unfortunately, the initial dissipation (and, hence, the value of ε_0/SK_0) is not known in many of the important experimental studies of homogeneous turbulence including that of Champagne, Harris, and Corrsin (1970).

In Figures 5-6, the time evolution of the turbulent kinetic energy and dissipation rate are shown for $\Omega/S = 0.25$ and the same initial condition of $\varepsilon_0/SK_0 = 0.496$. From Figures 5-6, it is clear that all of the models badly underpredict the turbulent kinetic energy and dissipation rate in comparison to the results of the large-eddy simulation of Bardina, Ferziger, and Reynolds (1983). This discrepancy appears to be serious since the rather dramatic increase in turbulence activity indicated by the large-eddy simulations in Figure 5 has been confirmed independently by linear spectral calculations (see Figure 3 in Bertoglio 1982). In addition, one would expect, on physical grounds, the case of $\Omega/S = 0.25$ to be substantially more energetic than the case of $\Omega/S = 0$. When third-order moments are neglected in the Reynolds stress transport equations, the equations associated with the $\Omega/S = 0.25$ case are identical to those for plane strain and it is well known that plane strain is considerably more energetic than plane shear in homogeneous turbulence.

The time evolution of the turbulent kinetic energy and dissipation rate for $\Omega/S = 0.5$ and an initial condition of $\varepsilon_0/SK_0 = 0.496$ is shown in Figures 7-8. It is ironic to note that the K$-\varepsilon$ model yields the best agreement with the results of large-eddy simulations for this case. However, it must be remembered that the K$-\varepsilon$ model has a major defect in that it predicts the same results for K and ε *independent* of the value of Ω/S – a state of affairs that is contrary to both physical and numerical experiments. The Launder, Reece, and

Rodi model and the Rotta-Kolmogorov model yield qualitatively different predictions for this case (the former model predicts that the turbulence decays whereas the latter model predicts a weak exponential growth). This considerable disparity in the the predictions of the two models arises from the term containing C_2 on the right-hand-side of Eq. (22) in the Launder, Reece, and Rodi model which destroys similitude with respect to the Richardson number (a similarity property which the Rotta-Kolmogorov model has). The Richardson number

$$Ri = \frac{-2\Omega(S - 2\Omega)}{S^2} \tag{61}$$

is zero for the two cases of $\Omega/S = 0$ and $\Omega/S = 0.5$. Here, the Rotta-Kolmogorov model yields the same results for both cases; the Launder, Reece, and Rodi model yields qualitatively different results for the two cases; and large-eddy simulations indicate that the two cases are quantitatively distinct but qualitatively similar. It should be noted that the prediction of a decaying turbulence for sufficiently large values of $\Omega/S > 0.5$ is physically correct and will be discussed later.

The equilibrium states associated with the K$-\varepsilon$ model for rotating shear flow were derived earlier in equations (8), (13), (20), and (21). In Table 1, the specific numerical values of the equilibrium anisotropy tensor b_{ij} and shear parameter SK/ε are given as a function of Ω/S for both the linear and nonlinear K$-\varepsilon$ models. It should be pointed out that these results were computed using the value of $C_\mu = 0.055$ which was recommended by Rodi (1972) for ratios of production to dissipation P/ε of the order of two or greater (for the problem at hand, $P/\varepsilon = 2$). The traditional value of $C_\mu = 0.09$ was used for the time evolution computations since it rigorously applies for $P/\varepsilon = 1$ (the mean between the initial value of $P/\varepsilon = 0$ and the equilibrium value of $P/\varepsilon = 2$) and thus constitutes a reasonable average for C_μ that is used in most engineering calculations where there is a temporally or spatially varying turbulence structure. It is clear that the equilibrium values shown in Table 1 for the linear K$-\varepsilon$ model are extremely poor in their prediction of the normal components of the anisotropy tensor. The nonlinear K$-\varepsilon$ model yields

dramatically improved predictions for these normal components of the anisotropy tensor (it should be noted that the large-eddy simulations tend to overpredict the anisotropy tensor due to problems with defiltering). However, both the linear and nonlinear K$-\varepsilon$ models yield equilibrium values of b_{12} and SK/ε which are the *same* for all values of Ω/S. While these predictions for SK/ε are reasonably good for $\Omega/S = 0$, they can be in serious error for other values of Ω/S. Specifically, for large values of Ω/S, a relaminarization of the flow would be anticipated on physical grounds where the turbulence decays in such a way that $(\varepsilon/SK)_\infty = 0$. Such a relaminarization would be expected since, when $\Omega/S > 1$, the Rossby number $(\varepsilon/2\Omega K)_\infty < 0.1$. A Taylor-Proudman reorganization of the flow to a two-dimensional state can then occur (see Tritton 1977), and the preponderance of evidence indicates that uniform shear flow is stable to large amplitude two-dimensional disturbances (see Patera and Orszag 1981). Therefore, any trend toward a two-dimensionalization would be accompanied by a relaminarization. Linear spectral models suggest that uniform shear flow is unstable for $Ri \leq 0$ (i.e., $0 \leq \Omega/S \leq 0.5$). Although precise bounds for the stability of uniform shear flow in a rotating framework have not been established, it is generally believed that this flow is stable for Richardson numbers that are somewhat greater than zero (e.g., for $Ri > 0.2$; see Bertoglio 1982). Hence, it is clear that $(SK/\varepsilon)_\infty$ must vary considerably with Ω/S in conflict with results predicted by the K$-\varepsilon$ model.

The equilibrium states associated with Launder, Reece, and Rodi model are solutions of the nonlinear algebraic equations (38)-(41). Nonzero values of $(\varepsilon/SK)_\infty$ occur for $-0.0904 < \Omega/S < 0.3761$ where the equilibrium states are given by

$$\left(\frac{\varepsilon}{SK}\right)_\infty = \pm\frac{2(2-C_2)}{(1+C_1)}\left[\frac{(1-C_2)(C_1+2C_2-1)}{12(2-C_2)^2} + \left(\frac{1-C_2}{2-C_2}\right)\frac{\Omega}{S} - \left(\frac{\Omega}{S}\right)^2\right]^{\frac{1}{2}} \tag{62}$$

$$(b_{12})_\infty = -\alpha\left(\frac{\varepsilon}{SK}\right)_\infty \tag{63}$$

$$\alpha = \frac{C_{\varepsilon 2}-1}{C_{\varepsilon 1}-1} \tag{64}$$

$$(b_{11})_\infty = \frac{2\alpha\left[(2-C_2)\frac{\Omega}{S} - \frac{2}{3}(1-C_2)\right]}{1-\alpha-C_1} \tag{65}$$

$$(b_{22})_\infty = \frac{-2\alpha\left[(2-C_2)\frac{\Omega}{S} - \frac{1}{3}(1-C_2)\right]}{1-\alpha-C_1} \tag{66}$$

$$(b_{33})_\infty = \frac{-\frac{2}{3}\alpha(1-C_2)}{1-\alpha-C_1} \tag{67}$$

where, by linear analysis, it can be shown that the upper branch $(\varepsilon/SK)_\infty > 0$ is a stable fixed point of the focus type; the lower branch $(\varepsilon/SK)_\infty$ is an unstable fixed point of the same type. Of course, realizability requires that $\varepsilon/SK > 0$. Thus, it is interesting to note that realizability is satisfied by this model through the presence of the unstable branch $(\varepsilon/SK)_\infty = 0$ which is an invariant plane (hence, realizable initial conditions ensure realizable solutions for all time). Equilibrium solutions for the Launder, Reece, and Rodi model where $(\varepsilon/SK)_\infty = 0$ and $(b_{12})_\infty = 0$ exist for all Ω/S and are of the form:

$$(\varepsilon/SK)_\infty = 0, \ (b_{12})_\infty = 0 \tag{68}$$

$$(b_{11})_\infty = \left[\frac{1-C_2}{2-C_2}\left(\frac{S}{\Omega}\right) - 1\right](b_{22})_\infty - \frac{2}{3}\left(\frac{S}{\Omega}\right)\left(\frac{1-C_2}{2-C_2}\right) \tag{69}$$

$$(b_{33})_\infty = -\left(\frac{S}{\Omega}\right)\left(\frac{1-C_2}{2-C_2}\right)(b_{22})_\infty + \frac{2}{3}\left(\frac{S}{\Omega}\right)\left(\frac{1-C_2}{2-C_2}\right) \tag{70}$$

where $(b_{22})_\infty$ is arbitrary.[§] Linear analysis also shows that this solution is an unstable saddle in the region $-0.0592 < \Omega/S < 0.3449$; numerical results indicate that this solution is actually unstable for the entire region $-0.0904 < \Omega/S < 0.3761$ where the alternate solution (62)-(67) is stable. The equilibrium solution (68)-(70) is a stable fixed point of the focus type for $\Omega/S < -0.0904$ and $\Omega/S > 0.3761$. Interestingly enough, there

[§]Computations, however, indicate that for any given value of Ω/S only one value of $(b_{22})_\infty$ is stable.

exists an additional branch of equilibrium solutions where $(\varepsilon/SK)_\infty = 0$ and $(b_{12})_\infty$ is nonzero for $-0.0592 < \Omega/S < 0.3449$; however, these solutions are saddles which are, of course, unstable and thus never observable computationally. A bifurcation diagram of these equilibrium solutions for the Launder, Reece, and Rodi model is shown in Figure 9 where we plot $(\varepsilon/SK)_\infty$ vs. Ω/S. Only *one* stable equilibrium solution exists for a given value of Ω/S. It should be noted that the equilibrium solutions for which $(\varepsilon/SK)_\infty > 0$ have a turbulent kinetic energy and dissipation rate that grow exponentially with time. The stable equilibrium solutions for which $(\varepsilon/SK)_\infty = 0$ can have a turbulence structure that either grows or decays with time. More specifically, numerical solutions of the Launder, Reece, and Rodi model indicated an exponential growth in the turbulent kinetic energy and dissipation rate for $-0.11 \leq \Omega/S \leq 0.39$; there was a decay in the turbulent kinetic energy and dissipation rate for $\Omega/S < -0.11$ and $\Omega/S > 0.39$.

The Rotta-Kolmogorov model has equilibrium solutions of a similar nature. Nonzero values of $(\varepsilon/SK)_\infty$ occur in the region $-0.0915 < \Omega/S < 0.5915$ for which the equilibrium states are given by:

$$\left(\frac{\varepsilon}{SK}\right)_\infty = \frac{\pm\left[\frac{1}{3}\left(1-\frac{B_1}{6A_1}\right)(1-3C_1)(E-3) - 2C_1 + 8\left(\frac{\Omega}{S}\right) - 16\left(\frac{\Omega}{S}\right)^2\right]^{\frac{1}{2}}}{B_1/6A_1 - 1 - 2/(E-3)} \tag{71}$$

$$(b_{12})_\infty = \frac{2}{E-3}\left(\frac{\varepsilon}{SK}\right)_\infty \tag{72}$$

$$(b_{11})_\infty = \frac{4\left[\frac{2}{3} - 2\left(\frac{\Omega}{S}\right)\right]}{(E-3)\left[1 - B_1/6A_1 + 2/(E-3)\right]} \tag{73}$$

$$(b_{22})_\infty = \frac{4\left[2\left(\frac{\Omega}{S}\right) - \frac{1}{3}\right]}{(E-3)\left[1 - B_1/6A_1 + 2/(E-3)\right]} \tag{74}$$

$$(b_{33})_\infty = \frac{-\frac{4}{3}}{(E-3)\left[1 - B_1/6A_1 + 2/(E-3)\right]} \tag{75}$$

where (as with the Launder, Reece, and Rodi model) analysis indicates that the positive branch $(\varepsilon/SK)_\infty > 0$ is a stable fixed point of the focus type and the negative branch $(\varepsilon/SK)_\infty < 0$ is an unstable fixed point of the same type. These branches of equilibria exist in conjunction with one where $(\varepsilon/SK)_\infty = 0$ and $(b_{12})_\infty = 0$ which is valid for all Ω/S and given by

$$(\varepsilon/SK)_\infty = 0, \quad (b_{12})_\infty = 0 \tag{76}$$

$$(b_{11})_\infty = \left(1 - \frac{1}{2}\frac{S}{\Omega}\right)(b_{22})_\infty - \frac{1}{3}\frac{S}{\Omega}(1 - 3C_1) \tag{77}$$

$$(b_{33})_\infty = -\left(2 - \frac{1}{2}\frac{S}{\Omega}\right)(b_{22})_\infty + \frac{1}{3}\frac{S}{\Omega}(1 - 3C_1) \tag{78}$$

where $(b_{22})_\infty$ can be arbitrary (computations, however, suggest that only one value of $(b_{22})_\infty$ is stable for any given value of Ω/S). Computations indicate that the equilibrium solution (76)-(78) is unstable for $-0.0915 < \Omega/S < 0.5915$ (by a linear analysis it can be shown that (76)-(78) is an unstable saddle for $0.0009 < \Omega/S < 0.4991$). The stability of this solution for $\Omega/S > 0.5915$ and for $\Omega/S < -0.0915$ was verified by numerical computations. It is interesting to note that (similar to the Launder, Reece, and Rodi model) the Rotta-Kolmogorov model has additional unstable equilibria where $(\varepsilon/SK)_\infty = 0$ but $(b_{12})_\infty$ is nonzero in the region $0.0009 < \Omega/S < 0.4991$. By linear analysis, these equilibrium solutions can be shown to be saddles which are unstable. A bifurcation diagram for the Rotta-Kolmogorov model is shown in Figure 10. It has the same structure as that for the Launder, Reece, and Rodi model (the two models are topologically equivalent from a dynamical systems standpoint). The primary difference between the two models is that the Rotta-Kolmogorov model predicts an equilibrium value of $(\varepsilon/SK)_\infty = 0$ with a decaying turbulent kinetic energy and dissipation rate for $\Omega/S > 0.61$ as compared to the corresponding range of $\Omega/S > 0.39$ predicted by the Launder, Reece, and Rodi model. In this regard, the Rotta-Kolmogorov model is superior since linear spectral models of tur-

bulence suggest that rotating homogeneous shear flow is unstable for $0 \leq \Omega/S \leq 0.5$. The Launder, Reece, and Rodi model is seriously in error in its prediction of a relaminarization for $0.39 < \Omega/S < 0.5$. On the other hand, for pure shear flow ($\Omega/S = 0$) the Launder, Reece, and Rodi model yields an equilibrium value for $(\varepsilon/SK)_\infty$ that is in much better agreement with the experiments of Tavoularis and Corrsin (1981) than the result predicted by the Rotta-Kolmogorov model (see Table 2). The fact that the Launder, Reece, and Rodi model deviates incorrectly from Richardson number similarity can be seen in the equilibrium values for the anisotropy tensor for $\Omega/S = 0.25$ shown in Table 2. The Launder, Reece, and Rodi model predicts that $b_{22} \approx -3b_{11}$ whereas large eddy simulations and supporting analogies with plane strain (see Bardina, Ferziger, and Reynolds 1983) indicate that $b_{11} \approx b_{22}$ as predicted by the Rotta-Kolmogorov model.

In Figures 11-12, the time evolution of the turbulent kinetic energy and dissipation rate are shown for the Launder, Reece, and Rodi model and the Rotta-Kolmogorov model for $\Omega/S = -0.25$ and $\varepsilon_0/SK_0 = 0.496$. Both models predict a comparable decay in turbulent kinetic energy and dissipation rate that are in qualitative agreement with the linear spectral calculations of Bertoglio (1982). The Launder, Reece, and Rodi model exhibits more pronounced oscillations than the Rotta-Kolmogorov model (oscillations are to be expected from these models since their fixed points are of the focus type).

In Figure 13, the time evolution of SK/ε is shown for the K$-\varepsilon$ model, the Launder, Reece, and Rodi model, the Rotta-Kolmogorov model, and the direct numerical simulations of Lee, Kim, and Moin (1987) corresponding to the initial condition of $SK_0/\varepsilon_0 = 50$ which constitutes a strong shear. The direct simulations of Lee, Kim, and Moin (1987) were done using the Rogallo code which for the weak shear case was shown by Rogallo (1981) to yield equilibrium values of SK/ε in the range of those predicted by the turbulence models we have been considering. Hence, the numerical simulations are indicative of the possibility of another stable equilibrium value of $(SK/\varepsilon)_\infty$ attracting initial conditions such that $SK_0/\varepsilon_0 \gg 1$. The recent experiments of Karnik and Tavoularis (1983) and Rohr, et

al. (1988) are supportive of the possibility of more than one fixed point in homogeneous turbulent shear flow. However, the issue still needs to be clarified.

The results shown in Figure 13 are suggestive of a potential problem concerning the applicability of the commonly used turbulence models to strong homogeneous turbulent shear flows. To further illustrate this point, the time evolution of the turbulent kinetic energy and dissipation rate are shown in Figures 14-15, for the Launder, Reece, and Rodi model and the Rotta-Kolmogorov model corresponding to the mild counter-rotation of $\Omega/S = -0.1$ and the strong initial shear condition of $SK_0/\varepsilon_0 = 50$. Both solutions are indicative of an exponential growth in turbulent kinetic energy and dissipation with large amplitude oscillations for $St < 50$. While one expects rotations to induce inertial oscillations (and, consequently, it does seem to be correct that the models have fixed points of the focus type), it appears that the large amplitudes of the oscillations shown in Figures 14-15 are unphysical. Such oscillations did not occur in the linear spectral calculations of Bertoglio (1982) for rotating shear flow and have not, to the best of our knowledge, been observed in any comparable flow configuration.

4. CONCLUSIONS

Four commonly used turbulence models have been tested for the problem of homogeneous turbulent shear flow in a rotating frame. Extensive comparisons between the predictions of the various models and the results of physical and numerical experiments have been made. The following definitive conclusions can be drawn:

1. The standard K$-\varepsilon$ model is highly deficient in that it yields solutions which are the same for *all* values of Ω/S contrary to numerical simulations of the Navier-Stokes equations. In particular, the model badly underpredicts the normal components of the anisotropy tensor for all values of Ω/S and does not account for the flow restabilization which occurs for most positive Richardson numbers.

2. The nonlinear K$-\varepsilon$ model yields dramatically improved predictions for the normal components of the anisotropy tensor that are in the correct range of the results of large-eddy simulations for $0 \leq \Omega/S \leq 0.5$ and physical experiments for $\Omega/S = 0$. However, the nonlinear model yields the same deficient predictions for K and ε as the standard K$-\varepsilon$ model.

3. The Launder, Reece, and Rodi model yields reasonably acceptable predictions for the equilibrium states for pure shear ($\Omega/S = 0$) despite the fact that its time evolution predictions for K and ε are no more accurate than those for the K$-\varepsilon$ model. The model erroneously predicts flow restabilization for negative Richardson numbers (i.e., for $0.39 < \Omega/S < 0.5$, $-0.17 < Ri < 0$). Consequently, the model yields extremely poor quantitative predictions of the turbulence structure for $0.25 \leq \Omega/S \leq 0.5$.

4. The Rotta-Kolmogorov model predicts unstable flow (i.e., unbounded growth in K and ε) for $-0.11 \leq \Omega/S \leq 0.61$ which is in partial agreement with numerical simulations and linear spectral analyses of the Navier-Stokes equations. Its predictions for the equilibrium anisotropy tensor are reasonable (except for b_{33} which is erroneously independent of Ω/S) but it yields poor quantitative results for the time

evolution of K and ε along with the equilibrium values of SK/ε. Furthermore, the model exhibits exact similitude with respect to the Richardson number which is not supported by large-eddy simulations. However, in this regard, it is still superior to the Launder, Reece, and Rodi model which deivates too strongly from Richardson number similarity.

Finally, we will make suggestions for the development of improved models. It is clear that the major deficiency with the nonlinear K$-\varepsilon$ model lies in its lack of an $(\varepsilon/SK)_\infty = 0$ fixed point and the lack of any dependence on Ω/S in the dissipation rate transport equation. This can be corrected by allowing $C_{\varepsilon 1}$ and $C_{\varepsilon 2}$ to be nonlinear functions of an appropriate flow invariant which reduces to $\varepsilon/\Omega K$ for rotating shear flow. With such a correction, the nonlinear K$-\varepsilon$ model could be a strong competitor to the commonly used second-order closure models. In order to improve the second-order closures, we propose that material frame-indifference in the limit of two-dimensional turbulence (which constitutes a geostrophic flow constraint that all of the models considered herein violate) be applied in the manner of Haworth and Pope (1986) and Speziale (1985). This should yield improved behavior in the low Rossby number limit and provide the possibility of an additional fixed point for the high shear rate case since this correction increases by one the degree of the nonlinearity in τ_{ij}. The implementation of these improvements and their evaluation based on a dynamical systems approach will be the subject of a future paper.

REFERENCES

Bardina, J., Ferziger, J. H., and Reynolds, W. C. 1983 Improved turbulence models based on large-eddy simulation of homogeneous, incompressible turbulent flows. *Stanford University Technical Report TF-19.*

Bertoglio, J. P. 1982 Homogeneous turbulent field within a rotating frame. *AIAA J.* **20**, 1175.

Champagne, F. H., Harris, V. G., and Corrsin, S. 1970 Experiments on nearly homogeneous turbulent shear flow. *J. Fluid Mech.* **41**, 81.

Hanjalic, K. and Launder, B. E. 1972 A Reynolds stress model of turbulence and its application to thin shear flows. *J. Fluid Mech.* **52**, 609.

Haworth, D. C. and Pope, S. B. 1986 A generalized Langevin model for turbulent flows. *Phys. Fluids* **29**, 387.

Karnik, V. and Tavoularis, S. 1983 The asymptotic development of nearly homogeneous turbulent shear flow. *Turbulent Shear Flows* **4**, (L. J. S. Bradbury, F. Durst, B. E. Launder, F. W. Schmidt, and J. H. Whitelaw, eds.) p. 14-18, Springer-Verlag.

Launder, B. E., Reece, G., and Rodi, W. 1975 Progress in the development of a Reynolds stress turbulence closure. *J. Fluid Mech.* **68**, 537.

Lee, M. J., Kim, J., and Moin, P. 1987 Turbulence structure at high shear rate. *Proceedings of the Sixth Symposium on Turbulent Shear Flows*, Toulouse, France.

Mellor, G. L. and Herring, H. J. 1973 A survey of mean turbulent field closure models. *AIAA J.* **11**, 590.

Mellor, G. L. and Yamada, T. 1974 A hierarchy of turbulence closure models for planetary boundary layers. *J. Atmos. Sci.* **31**, 1791.

Reynolds, W. C. 1987 Fundamentals of turbulence for turbulence modeling and simulation. *Lecture Notes for Von Karman Institute, AGARD Lecture Series No. 86*, North Atlantic Treaty Organization.

Rodi, W. 1972 The prediction of free turbulent boundary layers by use of a two-equation model of turbulence. *Ph.D. Thesis*, University of London.

Rogallo, R. S. 1981 Numerical experiments in homogeneous turbulence. *NASA Technical Memorandum 81315.*

Rohr, J. J., Itsweire, E. C., Helland, K. N., and Van Atta, C. W. 1988 An investigation of the growth of turbulence in a uniform mean shear flow. *J. Fluid Mech.* **187**, 1.

Speziale, C. G. 1985 Second-order closure models for rotating turbulent flows. *ICASE Report No. 85-49*, NASA Langley Research Center.

Speziale, C. G. 1987 On nonlinear $K - \ell$ and K$-\varepsilon$ models of turbulence. *J. Fluid Mech.* **178**, 459.

Speziale, C. G. 1988 Turbulence modeling in non-inertial frames of reference. *ICASE Report No. 88-18*, NASA Langley Research Center.

Tavoularis, S. 1985 Asymptotic laws for transversely homogeneous turbulent shear flows. *Phys. Fluids* **28**, 999.

Tavoularis, S. and Corrsin, S. 1981 Experiments in nearly homogeneous turbulent shear flows with a uniform mean temperature gradient. Part I. *J. Fluid Mech.* **104**, 311.

Tritton, D. J. 1977 *Physical Fluid Dynamics*, Van Nostrand.

Tucker, H. J. and Reynolds, A. J. 1968 The distortion of turbulence by irrotational plane strain. *J. Fluid Mech.* **32**, 657.

	Equilibrium Values	Linear K−ε Model	Nonlinear K−ε Model	Experiments	Large-Eddy Simulations
$\Omega/S = 0$	b_{11}	0	0.431	0.403	0.61
	b_{22}	0	-0.308	-0.295	-0.53
	b_{12}	-0.332	-0.332	-0.284	-0.29
	SK/ε	6.03	6.03	6.08	-
$\Omega/S = 0.25$	b_{11}	0	0.062	-	0.12
	b_{22}	0	0.062	-	0.09
	b_{12}	-0.332	-0.332	-	-0.70
	SK/ε	6.03	6.03	-	-
$\Omega/S = 0.5$	b_{11}	0	-0.308	-	-0.53
	b_{22}	0	0.431	-	0.50
	b_{12}	-0.332	-0.332	-	-0.20
	SK/ε	6.03	6.03	-	-

Table 1. Equilibrium results for homogeneous turbulent shear flow in a rotating frame: Comparison of the predictions of the K−ε model with the large eddy simulations of Bardina, Ferziger, and Reynolds (1983) and the experiments of Tavoularis and Corrsin (1981).

	Equilibrium Values	LRR Model	RK Model	Experiments	Large-Eddy Simulations
$\Omega/S = 0.0$	b_{11}	0.381	0.483	0.403	0.61
	b_{22}	-0.190	-0.241	-0.295	-0.53
	b_{12}	-0.369	-0.337	-0.284	-0.29
	SK/ε	5.42	3.71	6.08	-
$\Omega/S = 0.25$	b_{11}	-0.119	0.121	-	0.12
	b_{22}	0.310	0.121	-	0.09
	b_{12}	-0.415	-0.495	-	-0.70
	SK/ε	4.83	2.53	-	-
$\Omega/S = 0.5$	b_{11}	-0.24	-0.241	-	-0.53
	b_{22}	0.32	0.483	-	0.50
	b_{12}	0	-0.337	-	-0.20
	SK/ε	∞	3.71	-	-

Table 2. Equilibrium results for homogeneous turbulent shear flow in a rotating frame: Comparison of the predictions of the Launder, Reece, and Rodi model and the Rotta-Kolmogorov model with the large-eddy simulations of Bardina, Ferziger, and Reynolds (1983) and the experiments of Tavoularis and Corrsin (1981).

LIST OF FIGURES

Figure 1. Homogeneous turbulent shear flow in a rotating frame.

Figure 2. Time evolution of the turbulent kinetic energy for homogeneous shear flow: $\Omega/S = 0$, $\varepsilon_0/SK_0 = 0.496$; —— K–$\varepsilon$ model, - - - Rotta-Kolmogorov (RK) model, – – Launder, Reece, and Rodi (LRR) model, o Large-eddy simulation of Bardina, Ferziger, and Reynolds (1983).

Figure 3. Time evolution of the turbulent dissipation rate for homogeneous shear flow: $\Omega/S = 0$, $\varepsilon_0/SK_0 = 0.496$.

Figure 4. Time evolution of the turbulent kinetic energy for homogeneous shear flow: $\Omega/S = 0$; $\varepsilon_0/SK_0 = 0.35$ for the K–ε model; $\varepsilon_0/SK_0 = 0.28$ for the Launder, Reece, and Rodi model and the Rotta-Kolmogorov model; and $\varepsilon_0/SK_0 = 0.496$ for the large-eddy simulation of Bardina, Ferziger, and Reynolds (1983).

Figure 5. Time evolution of the turbulent kinetic energy for rotating homogeneous shear flow: $\Omega/S = 0.25$, $\varepsilon_0/SK_0 = 0.496$.

Figure 6. Time evolution of the turbulent dissipation rate for rotating homogeneous shear flow: $\Omega/S = 0.25$, $\varepsilon_0/SK_0 = 0.496$.

Figure 7. Time evolution of the turbulent kinetic energy for rotating homogeneous shear flow: $\Omega/S = 0.5$, $\varepsilon_0/SK_0 = 0.496$.

Figure 8. Time evolution of the turbulent dissipation rate for rotating homogeneous shear flow: $\Omega/S = 0.5$, $\varepsilon_0/SK_0 = 0.496$.

Figure 9. Bifurcation diagram for the Launder, Reece, and Rodi model.

Figure 10. Bifurcation diagram for the Rotta-Kolmogorov model.

Figure 11. Time evolution of the turbulent kinetic energy and dissipation rate for the Launder, Reece, and Rodi model: $\Omega/S = -0.25$, $\varepsilon_0/SK_0 = 0.496$.

Figure 12. Time evolution of the turbulent kinetic energy and dissipation rate for the Rotta-Kolmogorov model: $\Omega/S = -0.25$, $\varepsilon_0/SK_0 = 0.496$.

Figure 13. Time evolution of SK/ε for homogeneous turbulent shear flow ($\Omega/S = 0$, $SK_0/\varepsilon_0 = 50$): o Direct numerical simulations of Lee, Kim, and Moin (1987).

Figure 14. Time evolution of the turbulent kinetic energy and dissipation rate for the Launder, Reece, and Rodi model: $\Omega/S = -0.1$, $SK_0/\varepsilon_0 = 50$.

Figure 15. Time evolution of the turbulent kinetic energy and dissipation rate for the Rotta-Kolmogorov model: $\Omega/S = -0.1$, $SK_0/\varepsilon_0 = 50$.

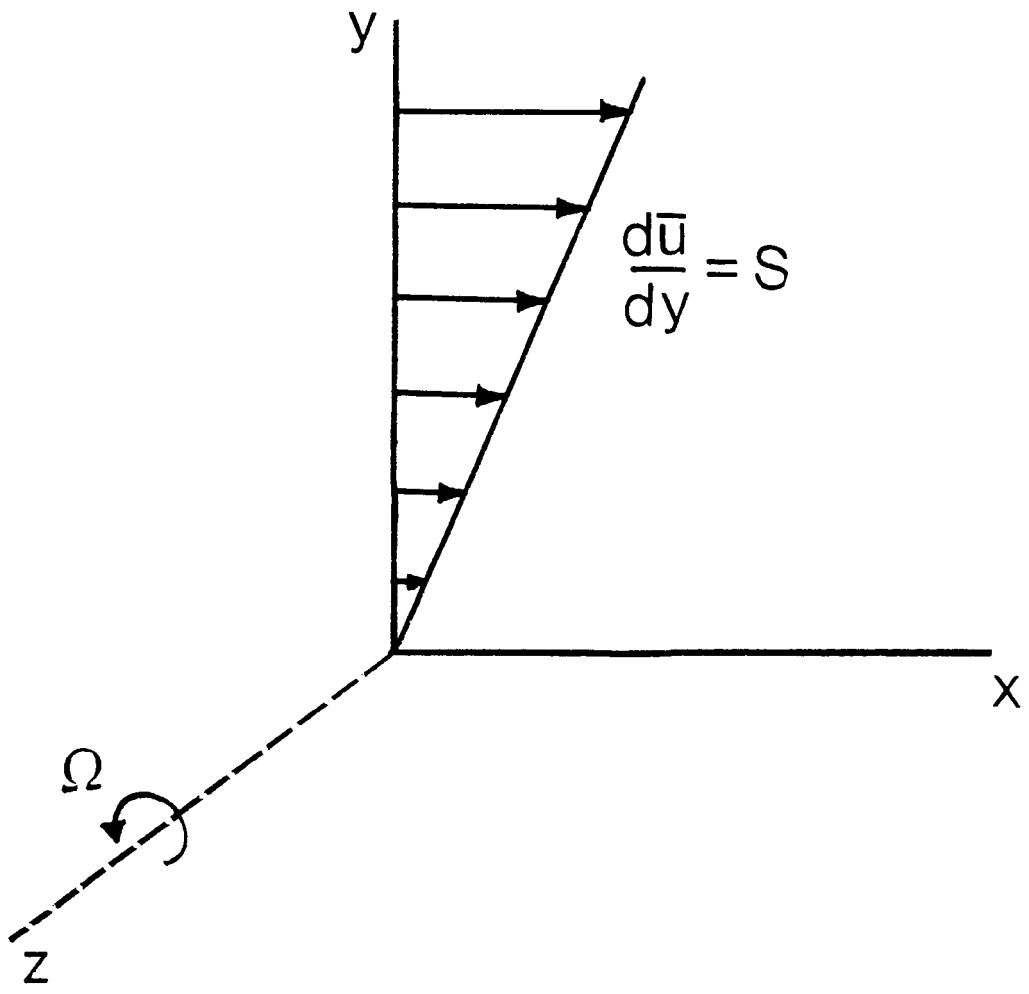

Figure 1. **Homogeneous turbulent shear flow in a rotating frame.**

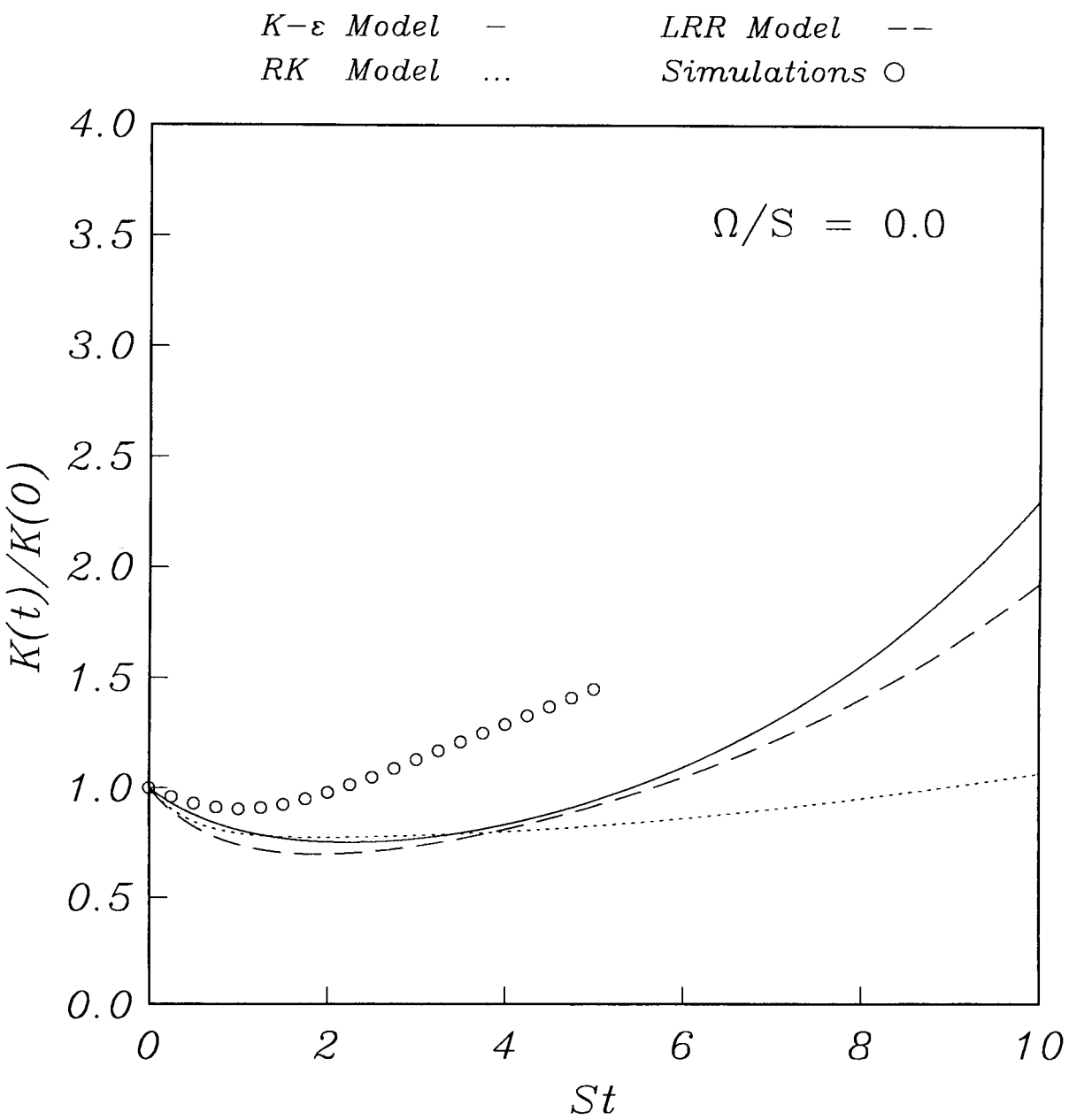

Figure 2. **Time evolution of the turbulent kinetic energy for homogeneous shear flow: $\Omega/S = 0$, $\epsilon_0/SK_0 = 0.496$; —— K−ϵ model, - - - Rotta-Kolmogorov (RK) model, – – Launder, Reece, and Rodi (LRR) model, o Large-eddy simulation of Bardina, Ferziger, and Reynolds (1983).**

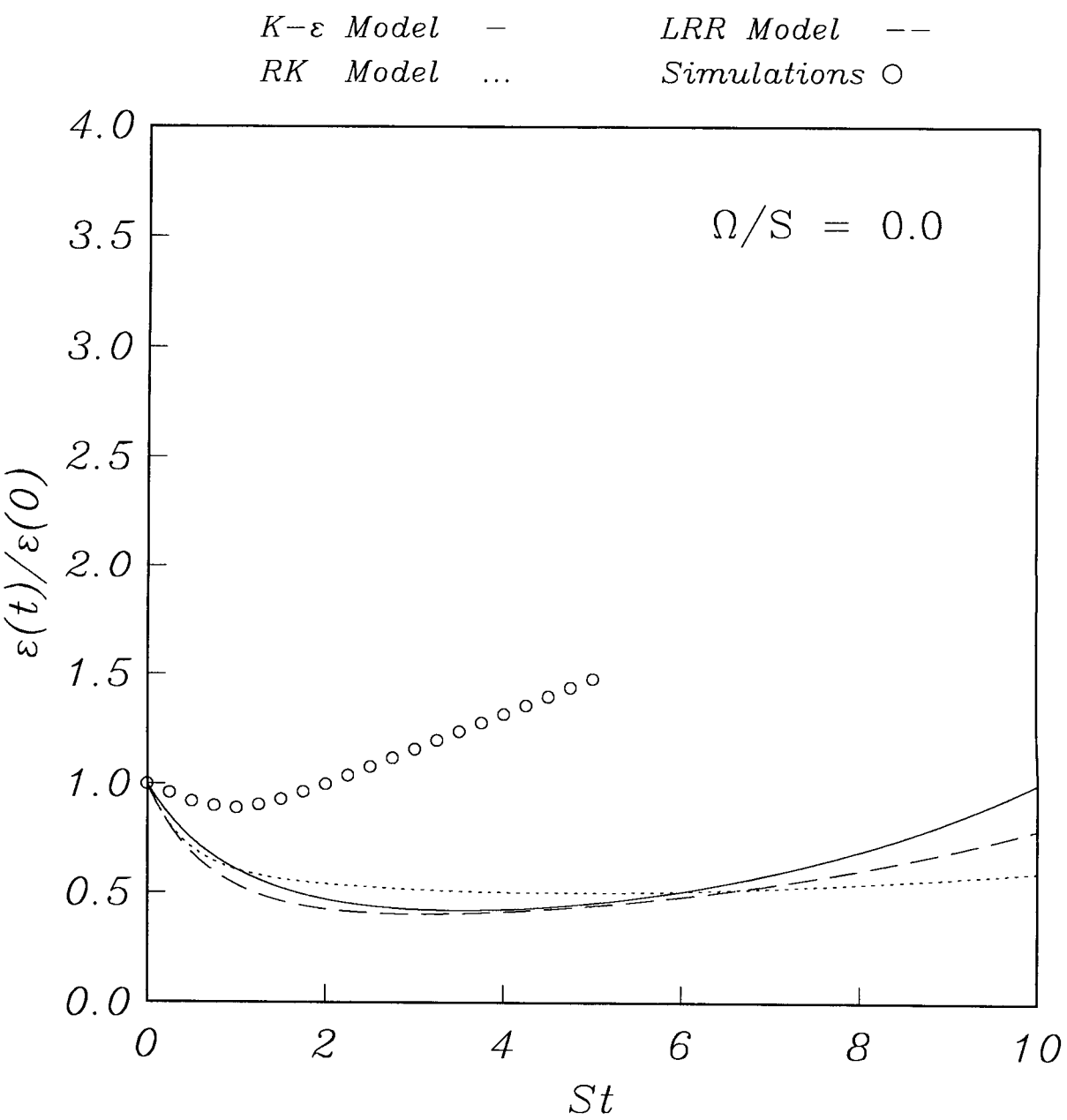

Figure 3. **Time evolution of the turbulent dissipation rate for homogeneous shear flow: $\Omega/S = 0$, $\varepsilon_0/SK_0 = 0.496$.**

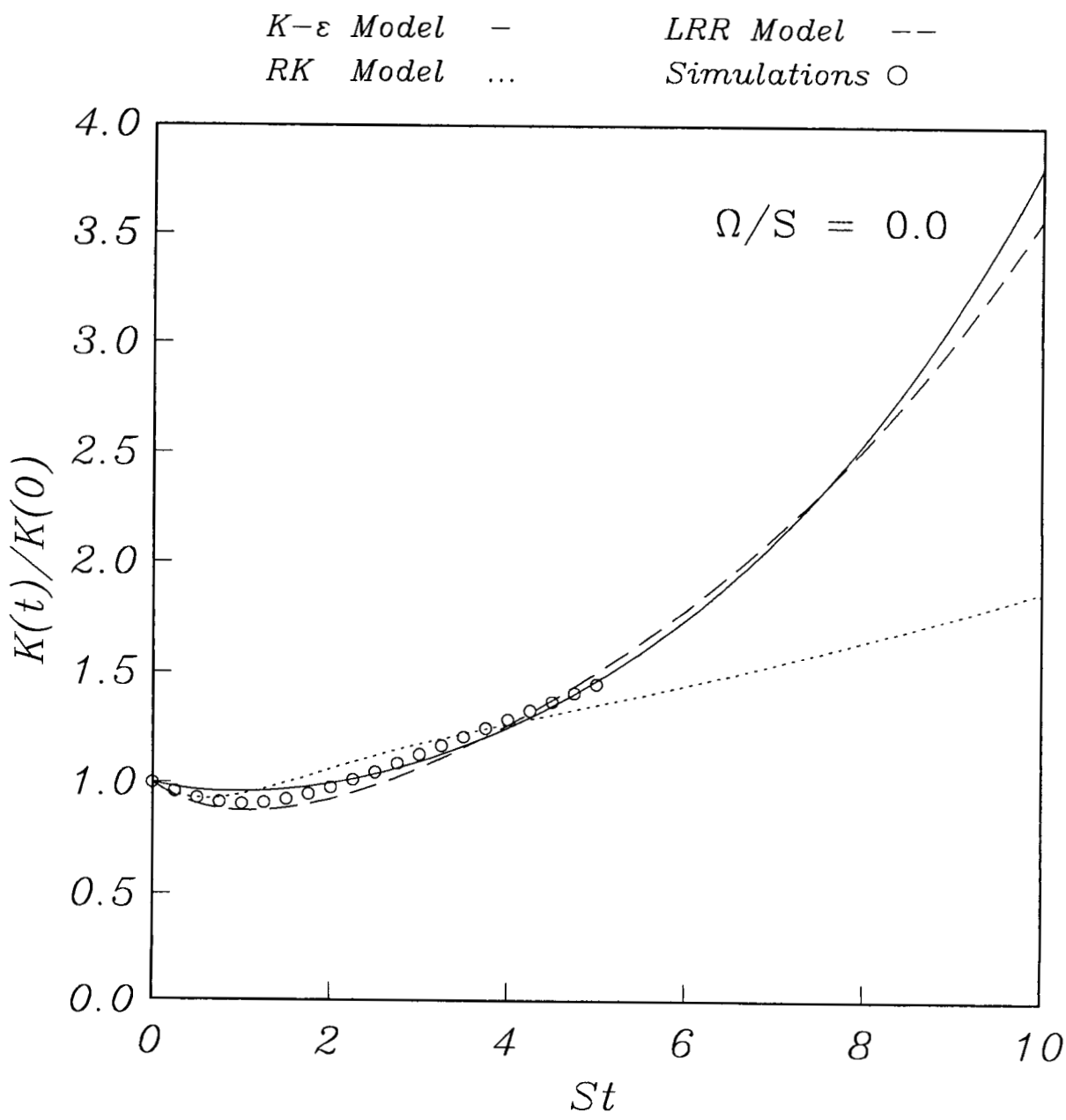

Figure 4. **Time evolution of the turbulent kinetic energy for homogeneous shear flow: $\Omega/S = 0$; $\varepsilon_0/SK_0 = 0.35$ for the K−ε model; $\varepsilon_0/SK_0 = 0.28$ for the Launder, Reece, and Rodi model and the Rotta-Kolmogorov model; and $\varepsilon_0/SK_0 = 0.496$ for the large-eddy simulation of Bardina, Ferziger, and Reynolds (1983).**

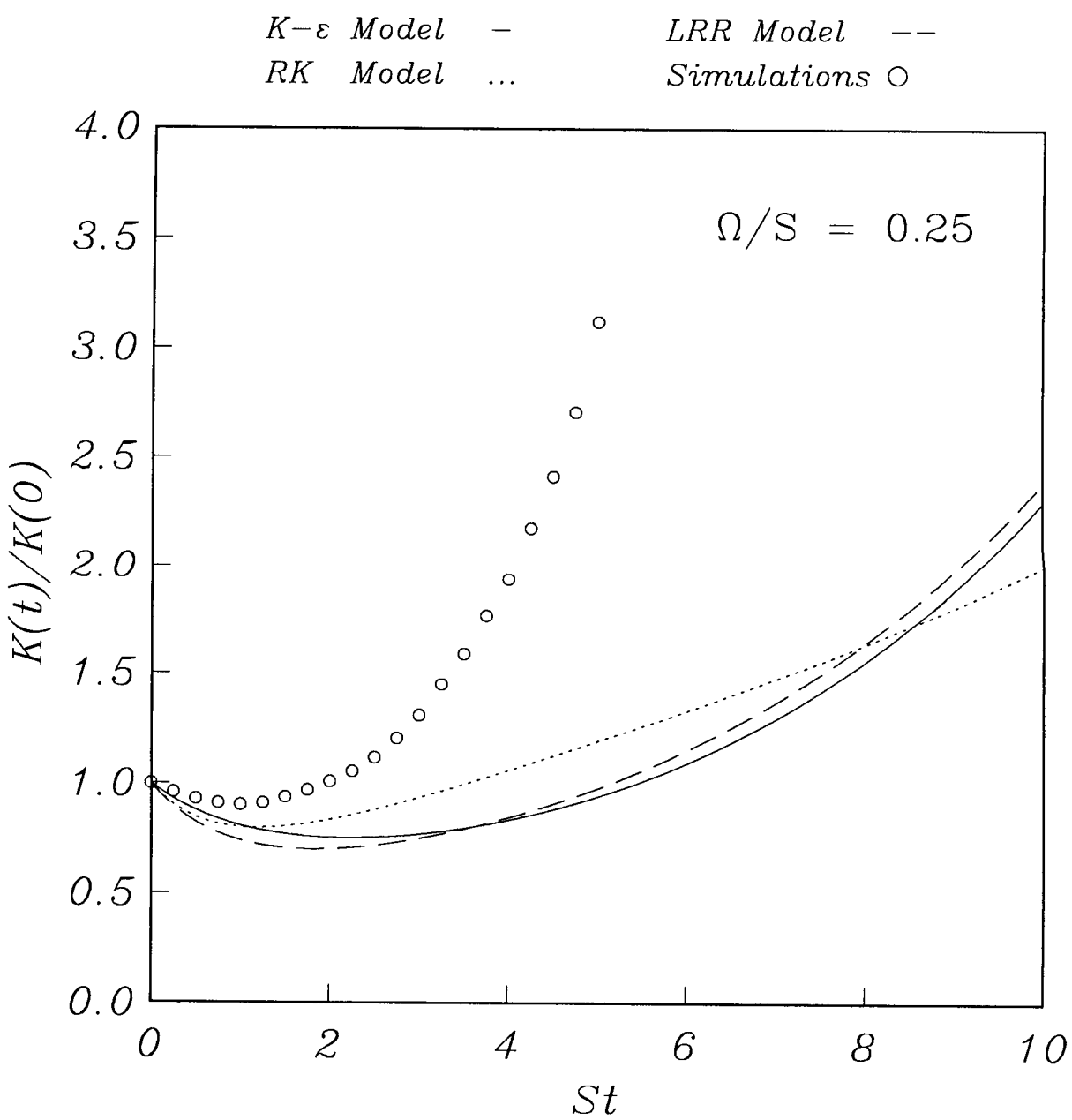

Figure 5. **Time evolution of the turbulent kinetic energy for rotating homogeneous shear flow: $\Omega/S = 0.25$, $\epsilon_0/SK_0 = 0.496$.**

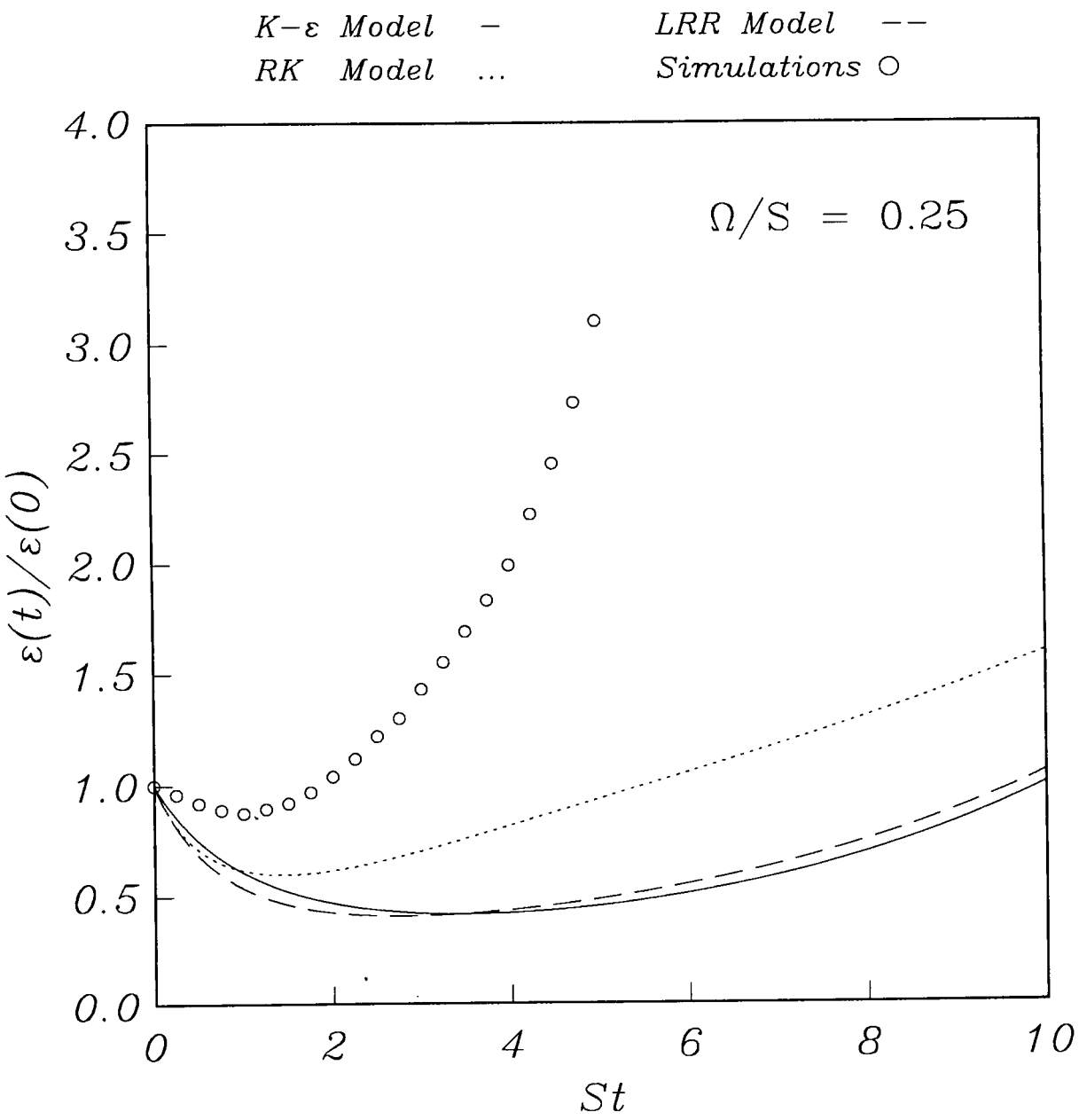

Figure 6. **Time evolution of the turbulent dissipation rate for rotating homogeneous shear flow: $\Omega/S = 0.25$, $\epsilon_0/SK_0 = 0.496$.**

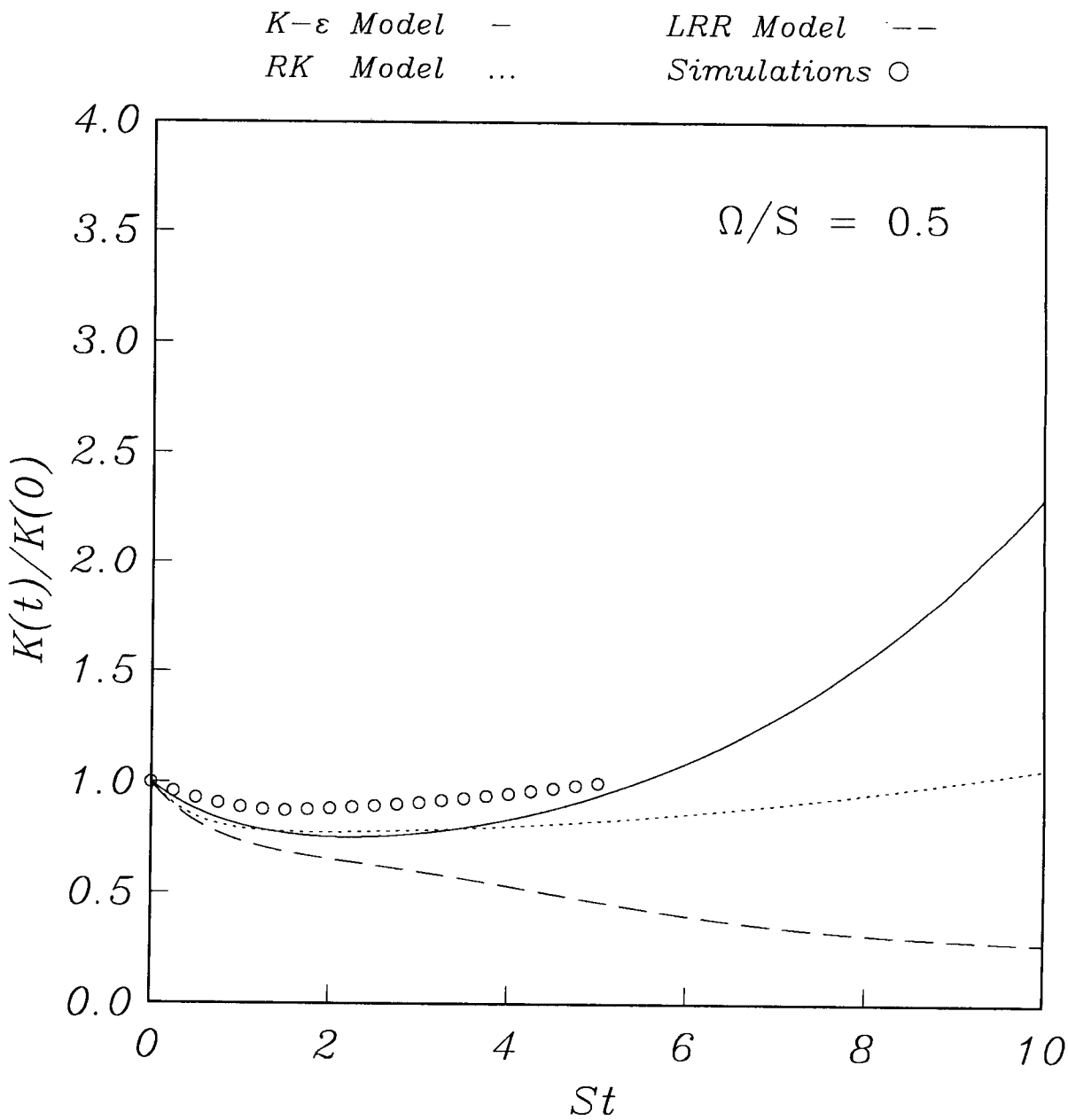

Figure 7. **Time evolution of the turbulent kinetic energy for rotating homogeneous shear flow: $\Omega/S = 0.5$, $\epsilon_0/SK_0 = 0.496$.**

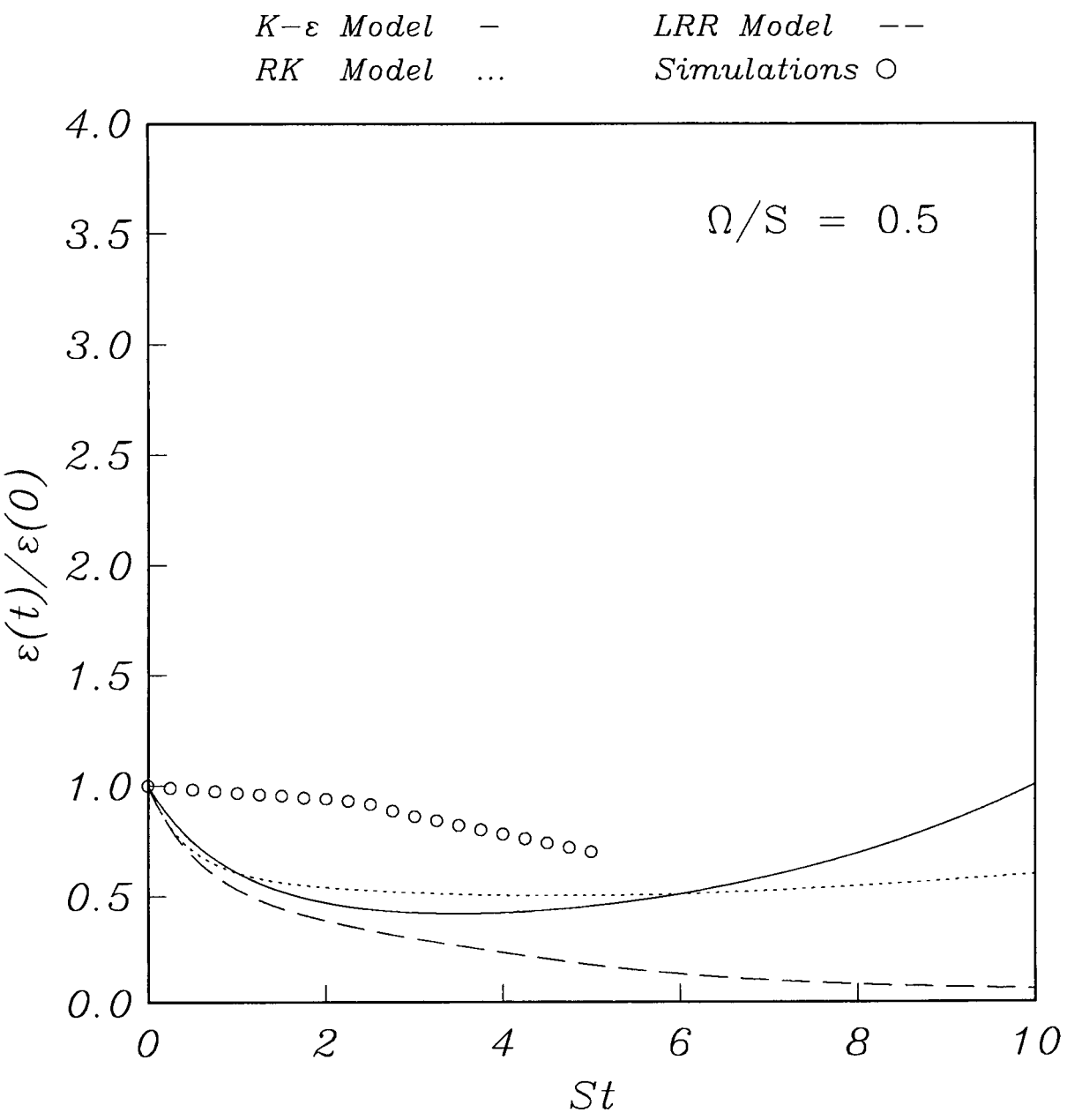

Figure 8. **Time evolution of the turbulent dissipation rate for rotating homogeneous shear flow: $\Omega/S = 0.5$, $\epsilon_0/SK_0 = 0.496$.**

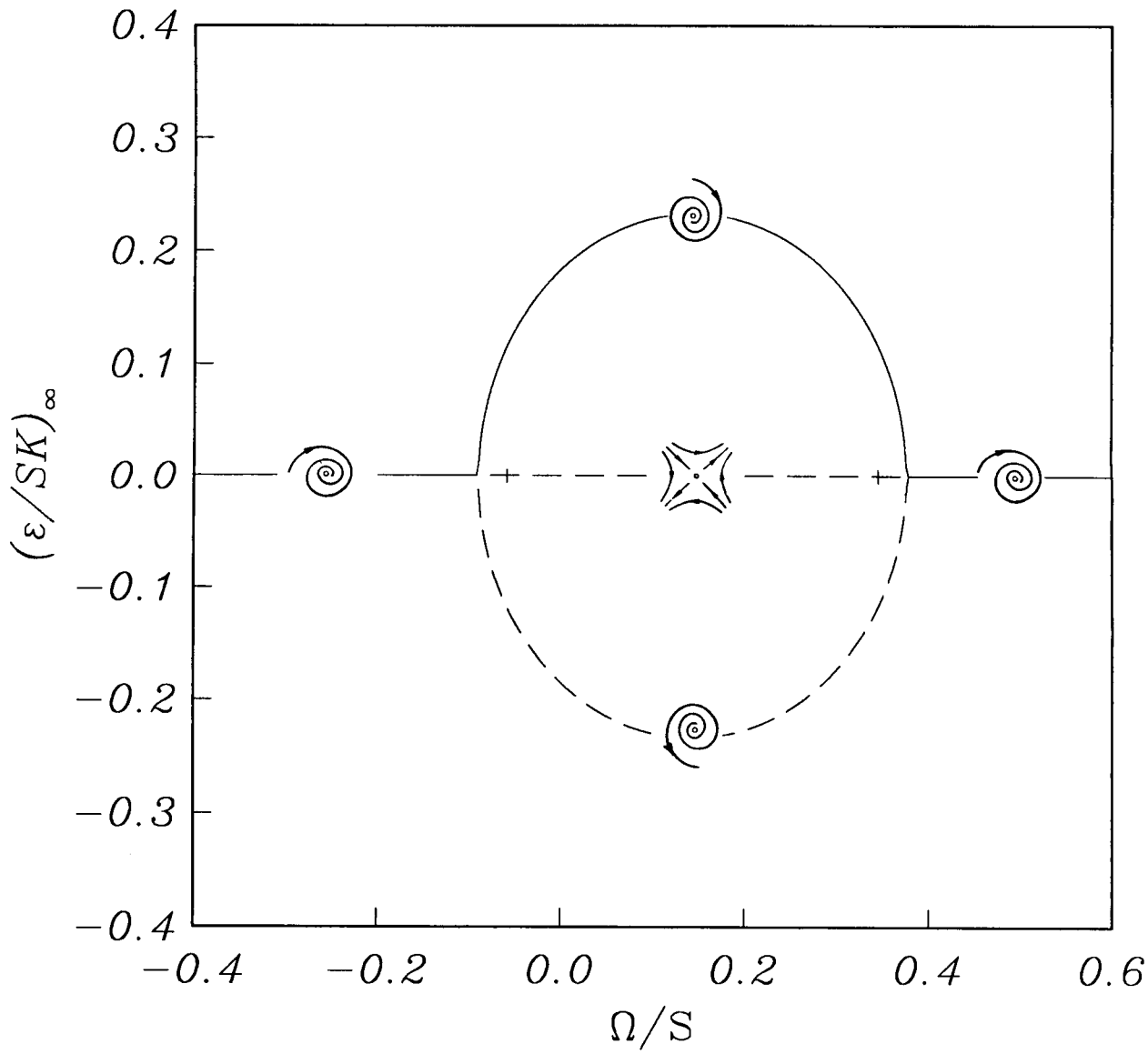

Figure 9. **Bifurcation diagram for the Launder, Reece, and Rodi model.**

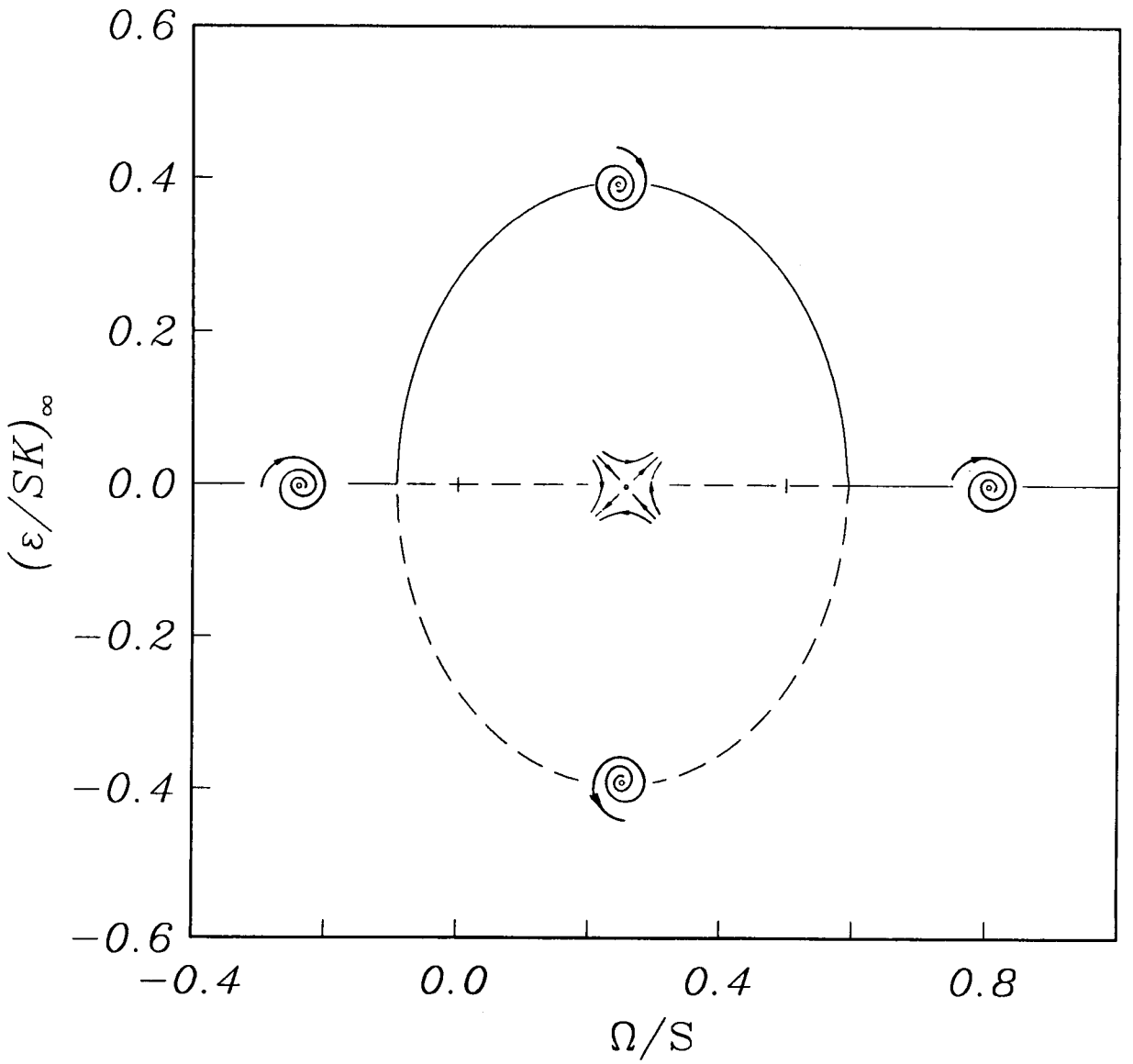

Figure 10. Bifurcation diagram for the Rotta-Kolmogorov model.

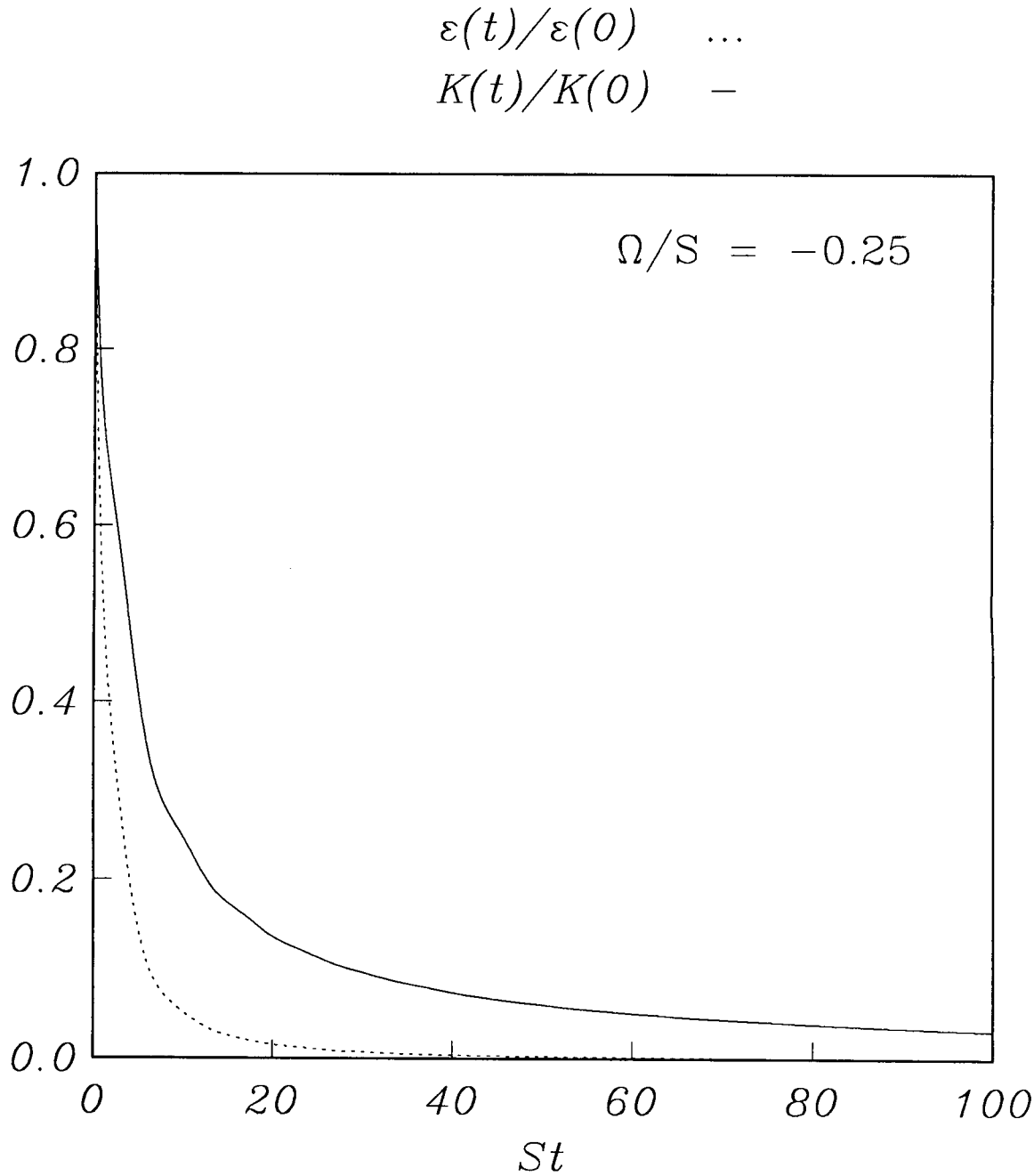

Figure 11. **Time evolution of the turbulent kinetic energy and dissipation rate for the Launder, Reece, and Rodi model: $\Omega/S = -0.25$, $\varepsilon_0/SK_0 = 0.496$.**

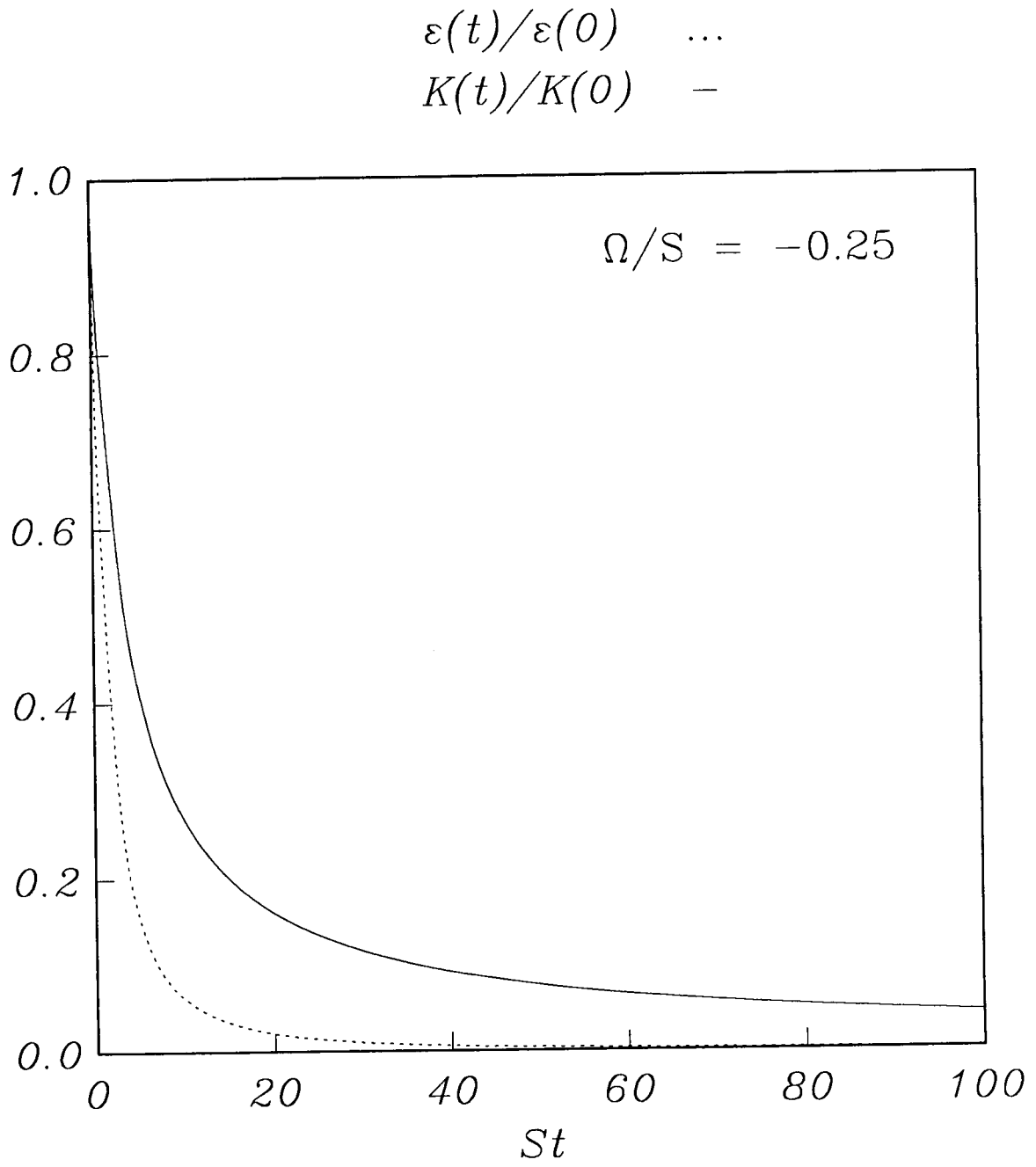

Figure 12. **Time evolution of the turbulent kinetic energy and dissipation rate for the Rotta-Kolmogorov model: $\Omega/S = -0.25$, $\varepsilon_0/SK_0 = 0.496$.**

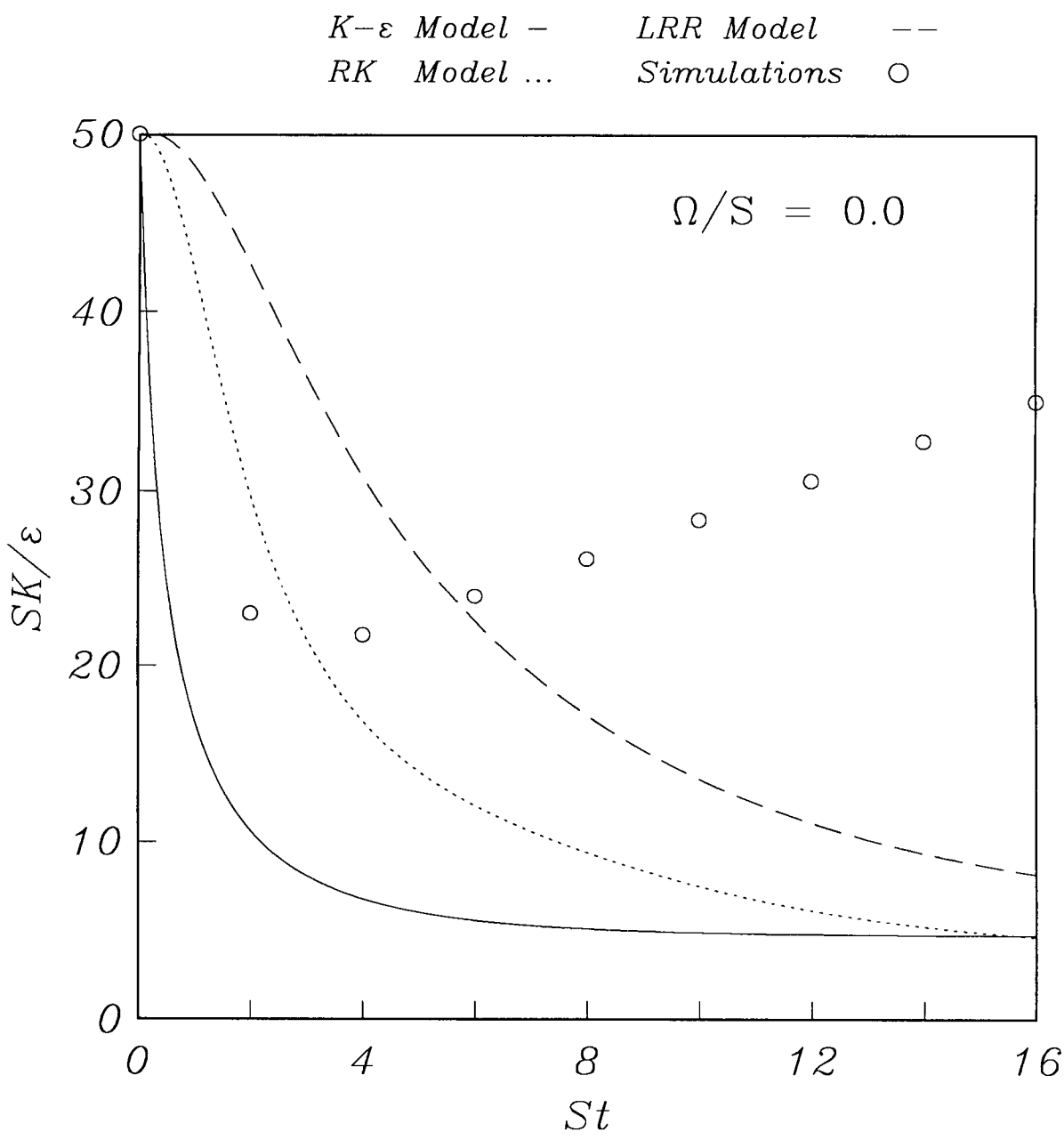

Figure 13. Time evolution of SK/ε for homogeneous turbulent shear flow ($\Omega/S = 0$, $SK_0/\varepsilon_0 = 50$): o Direct numerical simulations of Lee, Kim, and Moin (1987).

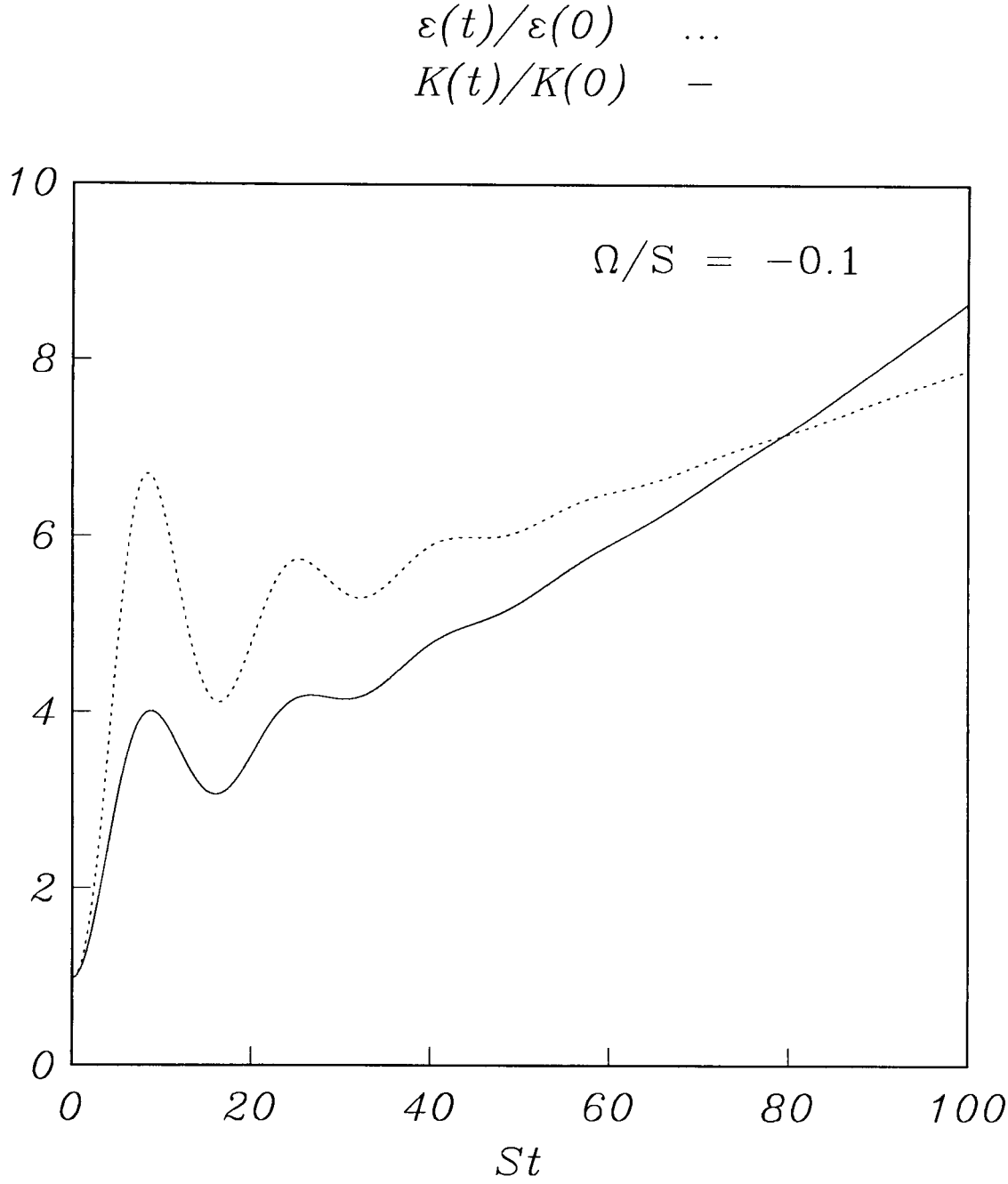

Figure 14. **Time evolution of the turbulent kinetic energy and dissipation rate for the Launder, Reece, and Rodi model: $\Omega/S = -0.1$, $SK_0/\varepsilon_0 = 50$.**

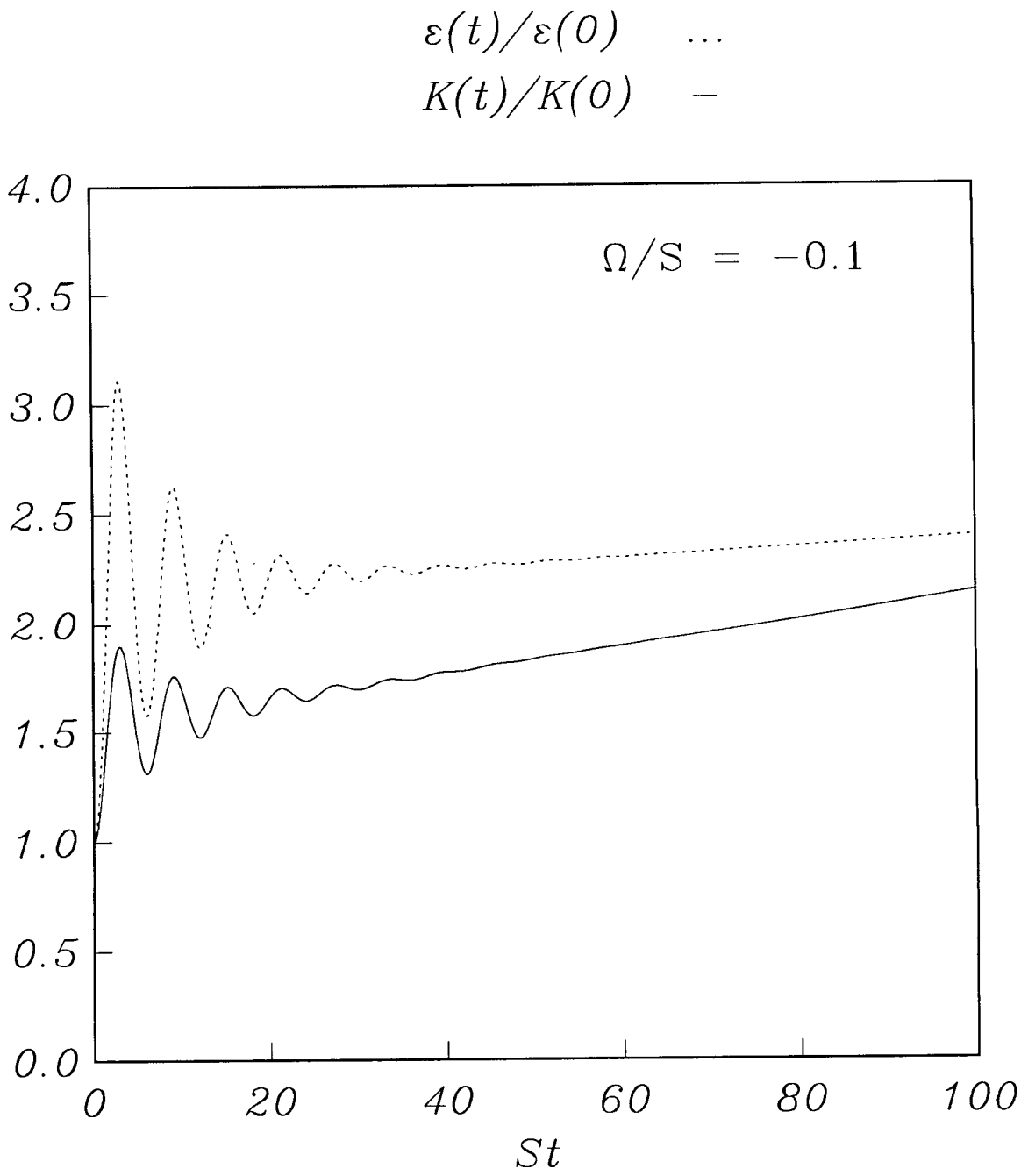

Figure 15. **Time evolution of the turbulent kinetic energy and dissipation rate for the Rotta-Kolmogorov model: $\Omega/S = -0.1$, $SK_0/\epsilon_0 = 50$.**

NASA
National Aeronautics and Space Administration

Report Documentation Page

1. Report No.	2. Government Accession No.	3. Recipient's Catalog No.
NASA CR-181659 ICASE Report No. 88-27		

4. Title and Subtitle	5. Report Date
ON THE PREDICTION OF EQUILIBRIUM STATES IN HOMOGENEOUS TURBULENCE	April 1988
	6. Performing Organization Code

7. Author(s)	8. Performing Organization Report No.
Charles G. Speziale and Nessan Mac Giolla Mhuiris	88-27
	10. Work Unit No. 505-90-21-01

9. Performing Organization Name and Address	11. Contract or Grant No.
Institute for Computer Applications in Science and Engineering Mail Stop 132C, NASA Langley Research Center Hampton, VA 23665-5225	NAS1-18107
	13. Type of Report and Period Covered: Contractor Report

12. Sponsoring Agency Name and Address	14. Sponsoring Agency Code
National Aeronautics and Space Administration Langley Research Center Hampton, VA 23665-5225	

15. Supplementary Notes

Langley Technical Monitor:
Richard W. Barnwell

Submitted to J. Fluid Mech.

Final Report

16. Abstract

A comparison of several commonly used turbulence models (including the $K-\varepsilon$ model and two second-order closures) is made for the test problem of homogeneous turbulent shear flow in a rotating frame. The time evolution of the turbulent kinetic energy and dissipation rate is calculated for a variety of models and comparisons are made with previously published experiments and numerical simulations. Particular emphasis is placed on examining the ability of each model to accurately predict equilibrium states for a range of the parameter Ω/S (the ratio of the rotation rate to the shear rate). It is found that none of the commonly used second-order closure models yield substantially improved predictions for the time evolution of the turbulent kinetic energy and dissipation rate over the somewhat defective results obtained from the simpler K$-\varepsilon$ model for the turbulent flow regime. There is also a problem with the equilibrium states predicted by the various models. For example, the K$-\varepsilon$ model erroneously yields equilibrium states that are independent of Ω/S while the Launder, Reece, and Rodi model predicts a flow relaminarization when $\Omega/S > 0.39$ – a result which is contrary to numerical simulations and linear spectral analyses which indicate flow instability for at least the range $0 \leq \Omega/S \leq 0.5$. The physical implications of the results obtained from the various turbulence models considered herein are discussed in detail along with proposals to remedy the deficiencies based on a dynamical systems approach.

17. Key Words (Suggested by Author(s))	18. Distribution Statement
homogeneous turbulence, rotating shear flow, K-ε model, second-order closure model	34 - Fluid Mechanics and Heat Transfer Unclassified - unlimited

19. Security Classif. (of this report)	20. Security Classif. (of this page)	21. No. of pages	22. Price
Unclassified	Unclassified	44	A03

NASA FORM 1626 OCT 86